

X(3872) and other possible heavy molecular states

Xiang Liu^{1,2,a}, Zhi-Gang Luo¹, Yan-Rui Liu³, Shi-Lin Zhu^{1,b}

¹Department of Physics, Peking University, Beijing 100871, China

²Centro de Física Computacional, Departamento de Física, Universidade de Coimbra, 3004-516, Coimbra, Portugal

³Institute of High Energy Physics, P.O. Box 918-4, Beijing 100049, China

Received: 14 November 2008 / Revised: 16 March 2009 / Published online: 8 April 2009

© Springer-Verlag / Società Italiana di Fisica 2009

Abstract We perform a systematic study of the possible molecular states composed of a pair of heavy mesons such as $D\bar{D}$, $D^*\bar{D}$, $D^*\bar{D}^*$ in the framework of the meson exchange model. The exchanged mesons include the pseudoscalar, scalar and vector mesons. Through our investigation, we find the following results. (1) The structure $X(3764)$ is not a molecular state. (2) There exists strong attraction in the range $r < 1$ fm for the $D^*\bar{D}^*$ system with $J = 0, 1$. If future experiments confirm $Z^+(4051)$ as a loosely bound molecular state, its quantum number is probably $J^P = 0^+$. Its partner state Φ^{**0} may be searched for in the $\pi^0\chi_{c1}$ channel. (3) Vector meson exchange provides strong attraction in the $D^*\bar{D}$ channel together with pion exchange. A bound state solution may exist with a reasonable cutoff parameter $\Lambda \sim 1.4$ GeV. $X(3872)$ may be accommodated as a molecular state dynamically although drawing a very definite conclusion needs further investigation. (4) The $B^*\bar{B}$ molecular state may exist.

PACS 12.39.Pn · 12.40.Yx · 13.75.Lb

1 Introduction

Since the observation of $Z^+(4430)$ [1], the Belle Collaboration reported two new resonance-like structures $Z^+(4051)$ and $Z^+(4248)$ in the $\pi^+\chi_{c1}$ mass distribution in the exclusive $\bar{B}^0 \rightarrow K^-\pi^+\chi_{c1}$ decay. Their masses and widths are $m_{Z^+(4051)} = (4051 \pm 14^{+20}_{-41})$ MeV, $\Gamma_{Z^+(4051)} = (82^{+21+47}_{-17-22})$ MeV and $m_{Z^+(4248)} = (4248 \pm 14^{+44+180}_{-29-35})$ MeV, $\Gamma_{Z^+(4248)} = (177^{+54+316}_{-39-61})$ MeV [2]. These charged hidden charm signals are good candidates of either tetraquark states or heavy molecular states if they are confirmed by future experiments.

^a e-mail: liuxiang@teor.fis.uc.pt

^b e-mail: zhuls@phy.pku.edu.cn

Recently the BES Collaboration reported an anomalous line-shape observed in the range of 3.650 GeV to 3.872 GeV by analyzing the cross section of $e^+e^- \rightarrow$ hadrons. The anomalous line-shape is composed of two possible enhancement structures around 3.764 GeV and 3.779 GeV respectively [3]. The latter one is consistent with the well-established $\psi(3770)$ while the mechanism of the first structure is not clear now, which is denoted $X(3764)$ in this work.

In the past five years, a series of observations of the charmonium-like X, Y, Z states, especially those states near the threshold of two charmed mesons have stimulated the interest in the possible existence of heavy molecular states greatly. The presence of the heavy quarks lowers the kinetic energy while the interaction between two light quarks could still provide strong enough attraction.

In fact, Voloshin and Okun studied the interaction between a pair of charmed mesons and proposed the possibilities of the molecular states involving charmed quarks more than thirty years ago [4]. De Rujula, Georgi and Glashow speculated on $\psi(4040)$ as a $D^*\bar{D}^*$ molecular state [5]. Törnqvist studied the possible deuteron-like two-meson bound states such as $D\bar{D}^*$ and $D^*\bar{D}^*$ using the quark-pion interaction model [6, 7]. Dubynskiy and Voloshin suggested the possibility of the existence of a new resonance at the $D^*\bar{D}^*$ threshold [8, 9]. Zhang, Chiang, Shen and Zou studied the possible S-wave bound states of two pseudoscalar mesons with vector meson exchange in [10]. The experimental observation of $X(3872)$ and $Z^+(4430)$ motivated the extensive discussion of $X(3872)$ as a $D\bar{D}^*$ molecular state [11–21] and $Z^+(4430)$ as a $D'_1 D^*(D_1 D^*)$ molecular state [22–27].

It's interesting to note that the $Z^+(4051)$ enhancement announced by the Belle collaboration and the $X(3764)$ signal reported by the BES collaboration are near the thresholds of $D^*\bar{D}^*$ and $D\bar{D}$ respectively. One may wonder whether they could also be candidates of heavy molecular states. In this work we perform a systematic study of three types of possible heavy molecular states: the $D\bar{D}/B\bar{B}$ system (P-P),

the $D^*\bar{D}^*/B^*\bar{B}^*$ system (V–V), and the $D^*\bar{D}/B^*\bar{B}$ system (P–V) using the formalism developed in [17, 18, 24–27].

This paper is organized as follows. After the introduction, we introduce some notations and present the flavor wave functions of the S-wave P–P, V–V and P–V systems constructed by two heavy flavor mesons. In Sect. 3, we collect the effective Lagrangians in the derivation of the effective potential. Sections 4–6 are for the P–P, V–V, P–V cases respectively. The last section is the discussion and conclusion.

2 Flavor wave functions of heavy molecular states

We study the possible molecular states composed of two pseudoscalar (P–P) heavy mesons, two vector (V–V) heavy mesons, one pseudoscalar and one vector (P–V) heavy mesons. The masses of the $J^P = 0^-, 1^-$ heavy mesons are taken from PDG [28] and collected in Table 1.

The P–P type is categorized as two systems, i.e. $\mathcal{D} - \bar{\mathcal{D}}$, $\mathcal{B} - \bar{\mathcal{B}}$. Here \mathcal{D} , $\bar{\mathcal{D}}$, \mathcal{B} and $\bar{\mathcal{B}}$ denote (D^0, D^+, D_s^+) , (\bar{D}^0, D^-, D_s^-) , (B^+, B^0, B_s^0) and $(B^-, \bar{B}^0, \bar{B}_s^0)$ triplets respectively. In the following, we illustrate their flavor wave functions with the $\mathcal{D} - \bar{\mathcal{D}}$ type as an example. Since charmed mesons belong to the fundamental representation of flavor SU(3), the $\mathcal{D} - \bar{\mathcal{D}}$ system form an octet and a singlet: $3 \otimes \bar{3} = 8 \oplus 1$. The corresponding flavor wave functions are $\Phi_s^+ = \bar{D}^0 D_s^+$, $\Phi^+ = \bar{D}^0 D^+$, $\Phi_s^0 = D^- D_s^+$, $\Phi^0 =$

$\frac{1}{\sqrt{2}}(\bar{D}^0 D^0 - D^- D^+)$, $\bar{\Phi}_s^0 = D_s^- D^+$, $\Phi_8^0 = \frac{1}{\sqrt{6}}(\bar{D}^0 D^0 + D^- D^+ - 2D_s^- D_s^+)$, $\Phi^- = D^- D^0$, $\Phi_s^- = D_s^- D^0$, $\Phi_1^+ = \frac{1}{\sqrt{3}}(\bar{D}^0 D^0 + D^- D^+ + D_s^- D_s^+)$. Through ideal mixing, we have $\Phi_8^0 = \frac{1}{\sqrt{2}}(\bar{D}^0 D^0 + D^- D^+)$ and $\Phi_{s1}^0 = D_s^- D_s^+$, where Φ_8^0 is an isoscalar while Φ^0 is an isovector. The above states are shown in Fig. 1 and collected in Table 2 together with the $\bar{\mathcal{B}} - \mathcal{B}$ type states. The flavor wave functions of the $D^*\bar{D}^*$ and $B^*\bar{B}^*$ systems are constructed similarly, which are denoted as Φ^{**} and Ω^{**} respectively.

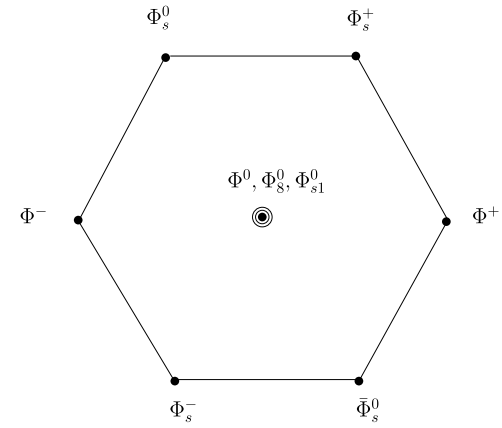


Fig. 1 The molecular multiplets composed of charmed and anti-charmed mesons

Table 1 The masses of heavy mesons in the H doublet [28]

J^P	Charmed-up(down) meson				Charmed-strange meson	
	Charged	Mass (MeV)	Neutral	Mass (MeV)	Charged	Mass (MeV)
0^-	D^\pm	1869.3	D^0	1864.5	D_s^\pm	1968.2
1^-	$D^{*\pm}$	2010.0	D^{*0}	2006.7	$D_s^{*\pm}$	2112.0
J^P Bottom-up(down) meson				Bottom-strange meson		
		Charged	Mass (MeV)	Neutral	Mass (MeV)	Neutral
0^-	B^\pm	5279.1	B^0	5279.5	B_s^0	5365.1
1^-	$B^{*\pm}$	5325.1	B^{*0}	5325.1	B_s^{*0}	5412.0

Table 2 The flavor wave functions of the $\mathcal{D} - \bar{\mathcal{D}}$ and $\mathcal{B} - \bar{\mathcal{B}}$ systems

State	$\mathcal{D} - \bar{\mathcal{D}}$ Wave function	State	$\bar{\mathcal{B}} - \mathcal{B}$ Wave function
Φ_s^+	$\bar{D}^0 D_s^+$	Ω_s^+	$B^+ \bar{B}_s^0$
Φ^+	$\bar{D}^0 D^+$	Ω^+	$B^+ \bar{B}^0$
Φ_s^0	$D^- D_s^+$	Ω_s^0	$B^0 \bar{B}_s^0$
Φ^0	$\frac{1}{\sqrt{2}}(\bar{D}^0 D^0 - D^- D^+)$	Ω^0	$\frac{1}{\sqrt{2}}(B^+ B^- - B^0 \bar{B}^0)$
$\bar{\Phi}_s^0$	$D_s^- D^+$	$\bar{\Omega}_s^0$	$B_s^0 \bar{B}^0$
Φ^-	$D^- D^0$	Ω^-	$B^0 B^-$
Φ_s^-	$D_s^- D^0$	Ω_s^-	$B_s^0 B^-$
Φ_8^0	$\frac{1}{\sqrt{2}}(\bar{D}^0 D^0 + D^- D^+)$	Ω_8^0	$\frac{1}{\sqrt{2}}(B^+ B^- + B^0 \bar{B}^0)$
Φ_{s1}^0	$D_s^- D_s^+$	Ω_{s1}^0	$B_s^0 \bar{B}_s^0$

Table 3 The flavor wave functions of the $\mathcal{D} - \bar{\mathcal{D}}^*$ and $\mathcal{B} - \bar{\mathcal{B}}^*$ systems

State	$\mathcal{D} - \bar{\mathcal{D}}^*$	State	$\mathcal{B} - \bar{\mathcal{B}}^*$
	Wave function		Wave function
$\Phi_s^{*+}/\hat{\Phi}_s^{*+}$	$\frac{1}{\sqrt{2}}(\bar{D}^{*0}D_s^+ + c\bar{D}^0D_s^{*+})$	$\Omega_s^{*+}/\hat{\Omega}_s^{*+}$	$\frac{1}{\sqrt{2}}(B^{*+}\bar{B}_s^0 + cB^+\bar{B}_s^{*0})$
$\Phi^{*+}/\hat{\Phi}^{*+}$	$\frac{1}{\sqrt{2}}(\bar{D}^{*0}D^+ + c\bar{D}^0D^{*+})$	$\Omega^{*+}/\hat{\Omega}^{*+}$	$\frac{1}{\sqrt{2}}(B^{*+}\bar{B}^0 + cB^+\bar{B}^{*0})$
$\Phi_s^{*0}/\hat{\Phi}_s^{*0}$	$\frac{1}{\sqrt{2}}(D^{*-}D_s^+ + cD^-D_s^{*+})$	$\Omega_s^{*0}/\hat{\Omega}_s^{*0}$	$\frac{1}{\sqrt{2}}(B^{*0}\bar{B}_s^0 + cB^0\bar{B}_s^{*0})$
$\Phi^{*0}/\hat{\Phi}^{*0}$	$\frac{1}{2}[(\bar{D}^{*0}D^0 - D^{*-}D^+) + c(\bar{D}^0D^{*0} - D^-D^{*+})]$	$\Omega^{*0}/\hat{\Omega}^{*0}$	$\frac{1}{2}[(B^{*+}B^- - B^{*0}\bar{B}^0) + c(B^+B^{*-} - B^0\bar{B}^{*0})]$
$\bar{\Phi}_s^{*0}/\hat{\bar{\Phi}}_s^{*0}$	$\frac{1}{\sqrt{2}}(D_s^{*-}D^+ + cD_s^-D^{*+})$	$\bar{\Omega}_s^{*0}/\hat{\bar{\Omega}}_s^{*0}$	$\frac{1}{\sqrt{2}}(B_s^{*0}\bar{B}^0 + cB_s^0\bar{B}^{*0})$
$\Phi^{*-}/\hat{\Phi}^{*-}$	$\frac{1}{\sqrt{2}}(D^{*-}D^0 + cD^-D^{*0})$	$\Omega_s^{*-}/\hat{\Omega}^{*-}$	$\frac{1}{\sqrt{2}}(B^{*0}B^- + cB^0B^{*-})$
$\Phi_s^{*-}/\hat{\Phi}_s^{*-}$	$\frac{1}{\sqrt{2}}(D_s^{*-}D^0 + cD_s^-D^{*0})$	$\Omega_s^{*-}/\hat{\Omega}_s^{*-}$	$\frac{1}{\sqrt{2}}(B_s^{*0}B^- + cB_s^0B^{*-})$
$\Phi_8^{*0}/\hat{\Phi}_8^{*0}$	$\frac{1}{2}[(\bar{D}^{*0}D^0 + D^{*-}D^+) + c(\bar{D}^0D^{*0} + D^-D^{*+})]$	$\Omega_8^{*0}/\hat{\Omega}_8^{*0}$	$\frac{1}{2}[(B^{*+}B^- + B^{*0}\bar{B}^0) + c(B^+B^{*-} + B^0\bar{B}^{*0})]$
$\Phi_{s1}^{*0}/\hat{\Phi}_{s1}^{*0}$	$\frac{1}{\sqrt{2}}(D_s^{*-}D_s^+ + cD_s^-D_s^{*+})$	$\Omega_{s1}^{*0}/\hat{\Omega}_{s1}^{*0}$	$\frac{1}{\sqrt{2}}(B_s^0\bar{B}_s^0 + cB_s^0\bar{B}_s^{*0})$

We label the $\mathcal{D} - \bar{\mathcal{D}}^*$ and $\mathcal{B} - \bar{\mathcal{B}}^*$ systems as Φ^* and Ω^* respectively and list their flavor wave function in Table 3. Here we need distinguish the C parity for Φ_s^{*0} , Φ_8^{*0} and Φ_{s1}^{*0} in the $\mathcal{D} - \bar{\mathcal{D}}^*$ system and Ω_s^{*0} , Ω_8^{*0} and Ω_{s1}^{*0} in the $\mathcal{B} - \bar{\mathcal{B}}^*$ system. The parameter $c = \mp 1$ corresponds to $C = \pm 1$ respectively as pointed out in [17, 18, 24, 25]. In this work we label those states with the negative charge parity with a hat such as $\hat{\Phi}^{*0}$, $\hat{\Phi}_8^{*0}$, $\hat{\Phi}_{s1}^{*0}$, $\hat{\Omega}^{*0}$, $\hat{\Omega}_8^{*0}$ and $\hat{\Omega}_{s1}^{*0}$. The charge parity of X(3872) is positive.

3 The Effective Lagrangian in the derivation of the potential

In the derivation of the potential, we need the effective Lagrangians, which are constructed based on the chiral symmetry and heavy quark symmetry [35–40]:

$$\mathcal{L} = ig \text{Tr}[H_b \gamma_\mu \gamma_5 A_{ba}^\mu \bar{H}_a] + i\beta \text{Tr}[H_b v^\mu (\mathcal{V}_\mu - \rho_\mu)_{ba} \bar{H}_a] + i\lambda \text{Tr}[H_b \sigma^{\mu\nu} F_{\mu\nu}(\rho) \bar{H}_a] + g_\sigma \text{Tr}[H_a \sigma \bar{H}_a], \quad (1)$$

where the field H is defined in terms of the $(0^-, 1^-)$ doublet

$$H_b = \frac{1+i}{2} [P_b^{*\mu} \gamma_\mu + i P_b \gamma_5]. \quad (2)$$

A_{ab}^μ is the axial vector field with definition

$$A_{ab}^\mu = \frac{1}{2} (\xi^\dagger \partial^\mu \xi - \xi \partial^\mu \xi^\dagger)_{ab} = \frac{i}{f_\pi} \partial^\mu \mathbb{P}_{ab} + \dots \quad (3)$$

with $\xi = \exp(i\mathbb{P}/f_\pi)$ and $f_\pi = 132$. The octet pseudoscalar and nonet vector meson matrices are

$$\mathbb{P} = \begin{pmatrix} \frac{\pi^0}{\sqrt{2}} + \frac{\eta}{\sqrt{6}} & \pi^+ & K^+ \\ \pi^- & -\frac{\pi^0}{\sqrt{2}} + \frac{\eta}{\sqrt{6}} & K^0 \\ K^- & \bar{K}^0 & -\frac{2\eta}{\sqrt{6}} \end{pmatrix}, \quad (4)$$

$$\mathbb{V} = \begin{pmatrix} \frac{\rho^0}{\sqrt{2}} + \frac{\omega}{\sqrt{2}} & \rho^+ & K^{*+} \\ \rho^- & -\frac{\rho^0}{\sqrt{2}} + \frac{\omega}{\sqrt{2}} & K^{*0} \\ K^{*-} & \bar{K}^{*0} & \phi \end{pmatrix}. \quad (5)$$

The effective interaction Lagrangians at the tree level from (1) are

$$\mathcal{L}_{\mathcal{D}\mathcal{D}\mathbb{V}} = -ig_{\mathcal{D}\mathcal{D}\mathbb{V}} (\mathcal{D}_a^\dagger \partial_\mu \mathcal{D}_b - \mathcal{D}_b \partial_\mu \mathcal{D}_a^\dagger) (\mathbb{V}^\mu)_{ab},$$

$$\mathcal{L}_{\mathcal{D}\mathcal{D}\sigma} = -2m_{\mathcal{D}} g_\sigma \mathcal{D}_a \mathcal{D}_a^\dagger \sigma,$$

$$\mathcal{L}_{\mathcal{D}^*\mathcal{D}^*\mathbb{P}} = \frac{1}{2} g_{\mathcal{D}^*\mathcal{D}^*\mathbb{P}} \varepsilon_{\mu\nu\alpha\beta} (D_a^{*\mu} \partial^\alpha D_b^{*\beta\dagger} - D_b^{*\mu} \partial^\alpha D_a^{*\beta\dagger}) \mathbb{P}_{ab},$$

$$\mathcal{L}_{\mathcal{D}^*\mathcal{D}^*\mathbb{V}} = ig_{\mathcal{D}^*\mathcal{D}^*\mathbb{V}} (\mathcal{D}_a^{*\nu\dagger} \partial^\mu \mathcal{D}_{v,b}^* - \mathcal{D}_{vb}^* \partial^\mu \mathcal{D}_a^{*\nu\dagger}) (\mathbb{V}_\mu)_{ab} + 4if_{\mathcal{D}^*\mathcal{D}^*\mathbb{V}} D_{\mu a}^{*\dagger} D_{vb}^* (\partial^\mu \mathbb{V}^\nu - \partial^\nu \mathbb{V}^\mu)_{ab},$$

$$\mathcal{L}_{\mathcal{D}^*\mathcal{D}^*\sigma} = 2m_{\mathcal{D}^*} g_\sigma \mathcal{D}_a^{*\alpha} \mathcal{D}_{aa}^{*\dagger} \sigma,$$

$$\mathcal{L}_{\mathcal{D}^*\mathcal{D}^*\mathbb{P}} = -ig_{\mathcal{D}^*\mathcal{D}^*\mathbb{P}} (\mathcal{D}_a \mathcal{D}_{\mu b}^{*\dagger} - \mathcal{D}_{\mu a}^* \mathcal{D}_b^\dagger) \partial^\mu \mathbb{P}_{ab},$$

$$\mathcal{L}_{\mathcal{D}^*\mathcal{D}^*\mathbb{V}} = -2f_{\mathcal{D}^*\mathcal{D}^*\mathbb{V}} \varepsilon_{\mu\nu\alpha\beta} (\partial^\mu \mathbb{V}^\nu)_{ab} [(\mathcal{D}_a^\dagger \partial^\alpha \mathcal{D}_b^{*\beta} - \partial^\alpha \mathcal{D}_a^\dagger \mathcal{D}_b^{*\beta}) - (\mathcal{D}_a^{*\beta\dagger} \partial^\alpha \mathcal{D}_b - \partial^\alpha \mathcal{D}_a^{*\beta\dagger} \mathcal{D}_b)],$$

where $\mathcal{D}^{(*)} = ((\bar{D}^0)^{(*)}, (D^-)^{(*)}, (D_s^-)^{(*)})$. The relevant coupling constants are

$$g_{\mathcal{D}^*\mathcal{D}^*\mathbb{P}} = \frac{g_{\mathcal{D}^*\mathcal{D}^*\mathbb{P}}}{\sqrt{m_{\mathcal{D}^*} m_{\mathcal{D}^*}}} = \frac{2g}{f_\pi},$$

$$g_{\mathcal{D}\mathcal{D}\mathbb{V}} = g_{\mathcal{D}^*\mathcal{D}^*\mathbb{V}} = \frac{\beta g_V}{\sqrt{2}},$$

$$f_{\mathcal{D}^*\mathcal{D}^*\mathbb{V}} = \frac{f_{\mathcal{D}^*\mathcal{D}^*\mathbb{V}}}{m_{\mathcal{D}^*}} = \frac{\lambda g_V}{\sqrt{2}},$$

$$g_V = \frac{m_\rho}{f_\pi}, \quad g_\sigma = \frac{g_\pi}{2\sqrt{6}},$$

where g_V , β and λ are parameters in the effective chiral Lagrangian that describe the interaction of heavy mesons with light vector mesons [39]. Following [41], we take $g = 0.59$, $\beta = 0.9$ and $\lambda = 0.56 \text{ GeV}^{-1}$. $g_\pi = 3.73$ [40].

In this work, we adopt the same formalism developed in [17, 18, 24–27] to derive the effective potential. We compute the amplitudes of the elastic scattering of two heavy mesons using the above effective Lagrangians. In order to account for the structure effect of every interaction vertex, we introduce the monopole type form factor (FF) [6, 7, 29–34]

$$F(q) = \frac{\Lambda^2 - m^2}{\Lambda^2 - q^2}. \quad (7)$$

Here q denotes the four-momentum of the exchanged meson. The quantity Λ is sometimes considered to have the value of approximately 1 GeV, but it may depend on the reduced mass of the system. It represents the inverse of a length scale, and the length scale for two light mesons differs from that for two very heavy mesons. The quantity Lambda also depends on the number and the nature of exchanged mesons, as the heavier exchanged mesons probe more of the short-distance behavior which interferes with the effect of the Lambda cut-off. In this work we adopt a universal cutoff to simplify the numerical analysis. The FF also plays the role of regularizing the potential by imposing a short-distance cutoff to cure the singularity of the effective potential. Then we impose the constraint that the initial states and final states should have the same angular momentum. After averaging the potentials obtained with the Breit approximation in the momentum space, we finally perform Fourier transformation to derive the potentials in the coordinate space. In the following sections, we illustrate the effective potentials in detail for the P–P, V–V and P–V systems.

4 The $\mathcal{D} - \bar{\mathcal{D}}$ case

4.1 The potential of the P–P system

The quantum number of the S-wave $\mathcal{D} - \bar{\mathcal{D}}$ system is $J^P = 0^+$ and the C parity of the neutral states is positive. In this work we consider the possible molecular states bound by the force from light pseudoscalar meson, vector meson and scalar exchange. Parity and angular momentum conservation forbid the exchange of a pseudoscalar meson between the $\mathcal{D} - \bar{\mathcal{D}}$ pair. No suitable meson exchange is allowed for the Φ_s^\pm and $\Phi_s^0(\bar{\Phi}_s^0)$ cases. For the other states, the effective potentials in the momentum space from vector meson and σ meson exchange are

$$\begin{aligned} \mathcal{V}_V(\mathbf{q}) & [I_1^{\mathbb{V}\mathcal{D}_1\mathcal{D}_1}, I_2^{\mathbb{V}\mathcal{D}_2\mathcal{D}_2}, m_{\mathcal{D}_1}, m_{\mathcal{D}_2}, m_V] \\ & = -g_{\mathcal{D}\mathcal{D}V}^2 I_1^{\mathbb{V}\mathcal{D}_1\mathcal{D}_1} I_2^{\mathbb{V}\mathcal{D}_2\mathcal{D}_2} \left(\frac{1}{\mathbf{q}^2 + m_V^2} + \frac{\mathbf{q}^2}{4m_{\mathcal{D}_1}m_{\mathcal{D}_2}m_V^2} \right), \end{aligned} \quad (8)$$

$$\mathcal{V}_\sigma(\mathbf{q}) = -g_\sigma^2 \frac{1}{\mathbf{q}^2 + m_\sigma^2}, \quad (9)$$

where $m_{\mathcal{D}}$ and m_V denote the masses of charmed meson and exchanged vector meson respectively. $I_1^{\mathbb{V}\mathcal{D}_1\mathcal{D}_1}$ and $I_2^{\mathbb{V}\mathcal{D}_2\mathcal{D}_2}$ arise from the coefficients related to the exchanged meson, which can be read from the nonet vector meson matrix in (5). After making the Fourier transformation, the three independent structures in (8)–(9) read

$$\mathbf{q}^2 \longrightarrow X(\Lambda, m, r), \quad (10)$$

$$\frac{1}{\mathbf{q}^2 + m^2} \longrightarrow Y(\Lambda, m, r), \quad (11)$$

$$\frac{\mathbf{q}^2}{\mathbf{q}^2 + m^2} \longrightarrow Z(\Lambda, m, r), \quad (12)$$

where

$$Y[\Lambda, m, r] = \frac{1}{4\pi r} (e^{-mr} - e^{-\Lambda r}) - \frac{\xi^2}{8\pi\Lambda} e^{-\Lambda r}, \quad (13)$$

$$Z[\Lambda, m, r] = -\frac{1}{r^2} \frac{\partial}{\partial r} \left(r^2 \frac{\partial}{\partial r} \right) Y[\Lambda, m, r], \quad (14)$$

$$X[\Lambda, m, r] = \left[-\frac{1}{r^2} \frac{\partial}{\partial r} \left(r^2 \frac{\partial}{\partial r} \right) + m^2 \right] Z[\Lambda, m, r] \quad (15)$$

with $\xi = \sqrt{\Lambda^2 - m^2}$. We have adopted the monopole FF in (7) to regularize the potential in (8)–(9). Now the effective potentials in the coordinate space read

$$\begin{aligned} \mathcal{V}_V(r) & [I_1^{\mathbb{V}\mathcal{D}_1\mathcal{D}_1}, I_2^{\mathbb{V}\mathcal{D}_2\mathcal{D}_2}, m_{\mathcal{D}_1}, m_{\mathcal{D}_2}, m_V] \\ & = -g_{\mathcal{D}\mathcal{D}V}^2 I_1^{\mathbb{V}\mathcal{D}_1\mathcal{D}_1} I_2^{\mathbb{V}\mathcal{D}_2\mathcal{D}_2} \left(Y[\Lambda, m_V, r] \right. \\ & \quad \left. + \frac{X[\Lambda, m_V, r]}{4m_{\mathcal{D}_1}m_{\mathcal{D}_2}m_V^2} \right), \end{aligned} \quad (16)$$

$$\mathcal{V}_\sigma(r) = -g_\sigma^2 Y[\Lambda, m_\sigma, r]. \quad (17)$$

The exchange potential for Φ^\pm in coordinate space is

$$\begin{aligned} \mathcal{V}(r)\Phi^\pm & = \mathcal{V}_V(r) \left[\frac{1}{\sqrt{2}}, -\frac{1}{\sqrt{2}}, m_{D^0}, m_{D^+}, m_{\rho^0} \right] \\ & \quad + \mathcal{V}_V(r) \left[\frac{1}{\sqrt{2}}, \frac{1}{\sqrt{2}}, m_{D^0}, m_{D^+}, m_\omega \right] + \mathcal{V}_\sigma(r) \\ & \approx -g_{\mathcal{D}\mathcal{D}V}^2 \left[\frac{Y[\Lambda, m_\omega, r]}{2} - \frac{Y[\Lambda, m_\rho, r]}{2} \right] \end{aligned}$$

$$-\frac{X[\Lambda, m_\rho, r]}{8m_D^2 m_\rho^2} + \frac{X[\Lambda, m_\omega, r]}{8m_D^2 m_\omega^2} \Big] \\ - g_\sigma^2 Y[\Lambda, m_\sigma, r]. \quad (18)$$

The symbol “ \approx ” means the SU(2) symmetry is assumed. For the Φ^0 and Φ_8^0 states, the exchange potentials are

$$\begin{aligned} \mathcal{V}(r)_{\text{Total}}^{\Phi^0(\Phi_8^0)} &= \frac{1}{2} \left\{ \mathcal{V}_V(r) \left[\frac{1}{\sqrt{2}}, \frac{1}{\sqrt{2}}, m_{D^0}, m_{D^0}, m_{\rho^0} \right] \right. \\ &\quad \mp 2\mathcal{V}_V(r) [1, 1, m_{D^0}, m_{D^+}, m_{\rho^\pm}] \\ &\quad + \mathcal{V}_V(r) \left[-\frac{1}{\sqrt{2}}, -\frac{1}{\sqrt{2}}, m_{D^+}, m_{D^-}, m_{\rho^0} \right] \\ &\quad + \mathcal{V}_V(r) \left[\frac{1}{\sqrt{2}}, \frac{1}{\sqrt{2}}, m_{D^0}, m_{D^0}, m_\omega \right] \\ &\quad + \mathcal{V}_V(r) \left[\frac{1}{\sqrt{2}}, \frac{1}{\sqrt{2}}, m_{D^+}, m_{D^-}, m_\omega \right] \\ &\quad \left. + 2\mathcal{V}_\sigma(r) \right\} \\ &\approx -\frac{g_{DDV}^2}{2} (1 \mp 2) \left(Y[\Lambda, m_\rho, r] \right. \\ &\quad \left. + \frac{X[\Lambda, m_\rho, r]}{4m_D^2 m_\rho^2} \right) - \frac{g_{DDV}^2}{2} \left(Y[\Lambda, m_\omega, r] \right. \\ &\quad \left. + \frac{X[\Lambda, m_\omega, r]}{4m_D^2 m_\omega^2} \right) - g_\sigma^2 Y[\Lambda, m_\sigma, r]. \quad (19) \end{aligned}$$

Clearly the potential of Φ_0 is the same as that of Φ^\pm due to the SU(2) symmetry. The effective potential of Φ_{s1}^0 is

$$\begin{aligned} \mathcal{V}(r)_{\text{Total}}^{\Phi_{s1}^0} &= \mathcal{V}_V(r) [1, 1, m_{D_s}, m_{D_s}, m_\phi] \\ &= -g_{DDV}^2 \left(Y[\Lambda, m_\phi, r] + \frac{X[\Lambda, m_\phi, r]}{4m_{D_s}^2 m_\phi^2} \right), \quad (20) \end{aligned}$$

where only ϕ meson exchange is allowed.

4.2 Numerical results for the P-P system

The input parameters include the coupling constants in (6), the masses of heavy mesons listed in Table 1, and the exchanged meson masses $m_\pi = 139.5$, $m_\rho = 775.5$, $m_\sigma = 600$, $m_\eta = 547.5$, $m_\omega = 782.7$ and $m_\phi = 1019.5$.

We first plot the variation of the effective potentials of the $D - \bar{D}$ system with the cutoff $\Lambda = 1$ GeV in Fig. 2. For the $\Phi^\pm(\Phi^0)$ state, there exist ρ , ω and σ meson exchanges. The ρ exchange force is repulsive while both the ω and σ meson exchange forces are attractive. The ρ and ω exchange forces cancel each other almost exactly. Thus the total potential is attractive. For the state Φ_{s1}^0 , the ϕ meson exchange potential is attractive. The exchange potentials of ρ , ω and σ mesons all are attractive for Φ_8^0 . Thus its total effective potential is attractive.

We adopt the MATSLISE package to solve the Schrödinger equation with the effective potentials of $\Phi^\pm(\Phi^0)$, Φ_{s1}^0 and Φ_8^0 states. MATSLISE is a graphical Matlab software package for the numerical study of regular Sturm-Liouville problems, one-dimensional Schrödinger equations and radial Schrödinger equations with a distorted coulomb potential. It allows for the fast and accurate computation of the eigenvalues and the visualization of the corresponding eigenfunctions [42–44].

The variation of binding energy E and the root-mean-square radius r_{rms} (in the unit of fm) of Φ_{s1}^0 , Φ_8^0 , Ω_{s1}^0 , Ω_8^0 with Λ is presented in Fig. 3, if there exists the solution by solving Schrödinger equation. For $\Phi^\pm(\Phi^0)$, we can not find bound state solutions in the range of $\Lambda < 10$ GeV, which indicates $\Phi^\pm(\Phi^0)$ does not exist. For both Φ_{s1}^0 and Φ_8^0 , there exist bound state solutions with Λ around 0.5 GeV. When the binding energy E becomes smaller, the r_{rms} becomes larger. Similar observations hold for the $B - \bar{B}$ system. Now the reduced masses of Ω_{s1}^0 and Ω_8^0 are heavier. Hence the kinetic term is smaller. Ω_{s1}^0 and Ω_8^0 states appear with a larger Λ around 1.1 GeV. In Fig. 3, we increase and reduce both the vector coupling constant and scalar coupling constant by a factor of two to see the variation of the binding energy and the cutoff parameter.

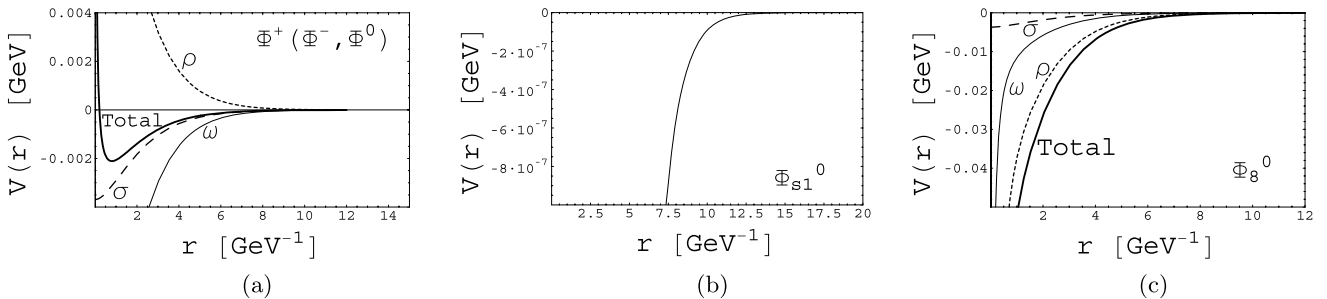


Fig. 2 Diagrams (a), (b) and (c) give respectively the variation of potentials of $\Phi^\pm(\Phi^0)$, Φ_{s1}^0 and Φ_8^0 states on r . Here we take the cutoff $\Lambda = 1$ GeV

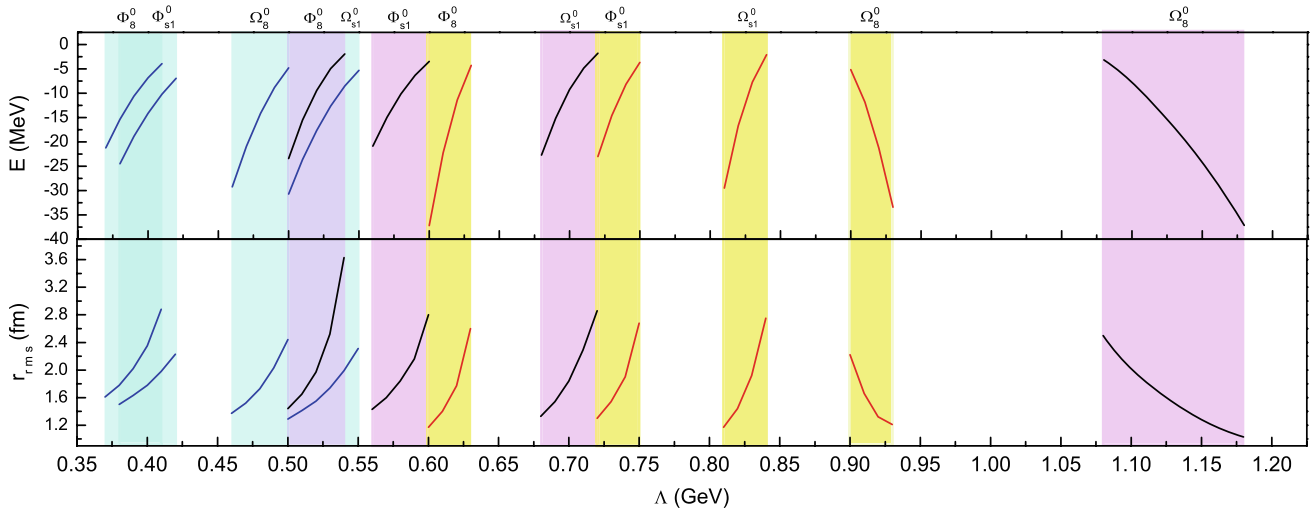


Fig. 3 (Color online) The dependence of binding energy E and the root-mean-square radius r_{rms} on Λ for Φ_{s1}^0 , Φ_8^0 , Ω_{s1}^0 , Ω_8^0 is marked by the red shadow band with the coupling constants in the text. The

yellow and blue shadow bands correspond to the cases when both the vector and scalar coupling constants are increased and reduced by a factor of two respectively

5 The $\mathcal{D}^* - \bar{\mathcal{D}}^*$ case

5.1 The potential of the V–V system

The possible quantum numbers of the S-wave V–V system are $J^P = 1^+, 1^+, 2^+$. The C parity is + for the neutral states. The exchanged mesons include the pseudoscalar, vector and σ mesons. The exchange potential reads

$$\begin{aligned} \mathcal{V}_{\mathbb{P}}^{[J]}(\mathbf{q}) & [I_1^{\mathbb{P}\mathcal{D}_1^*\mathcal{D}_1^*}, I_2^{\mathbb{P}\mathcal{D}_2^*\mathcal{D}_2^*}, m_{\mathcal{D}_1^*}, m_{\mathcal{D}_2^*}, m_{\mathbb{P}}] \\ & = \frac{1}{4} g_{\mathcal{D}^*\mathcal{D}^*\mathbb{P}}^2 I_1^{\mathbb{P}\mathcal{D}_1^*\mathcal{D}_1^*} I_2^{\mathbb{P}\mathcal{D}_2^*\mathcal{D}_2^*} \mathcal{A}[J] \frac{\mathbf{q}^2}{\mathbf{q}^2 + m_{\mathbb{P}}^2} \end{aligned} \quad (21)$$

for pseudoscalar meson exchange and

$$\begin{aligned} \mathcal{V}_{\mathbb{V}}^{[J]}(\mathbf{q}) & [I_1^{\mathbb{V}\mathcal{D}_1^*\mathcal{D}_1^*}, I_2^{\mathbb{V}\mathcal{D}_2^*\mathcal{D}_2^*}, m_{\mathcal{D}_1^*}, m_{\mathcal{D}_2^*}, m_{\mathbb{V}}] \\ & = -I_1^{\mathbb{V}\mathcal{D}_1^*\mathcal{D}_1^*} I_2^{\mathbb{V}\mathcal{D}_2^*\mathcal{D}_2^*} \\ & \times \left[\frac{g_{\mathcal{D}^*\mathcal{D}^*\mathbb{V}}^2}{4m_{\mathcal{D}_1^*}m_{\mathcal{D}_2^*}} \mathcal{C}[J] \frac{\mathbf{q}^2}{m_{\mathbb{V}}^2} + g_{\mathcal{D}^*\mathcal{D}^*\mathbb{V}}^2 \mathcal{C}[J] \frac{1}{\mathbf{q}^2 + m_{\mathbb{V}}^2} \right. \\ & \left. + \frac{4f_{\mathcal{D}^*\mathcal{D}^*\mathbb{V}}^2}{m_{\mathcal{D}_1^*}m_{\mathcal{D}_2^*}} \mathcal{B}[J] \frac{\mathbf{q}^2}{\mathbf{q}^2 + m_{\mathbb{V}}^2} \right] \end{aligned} \quad (22)$$

for vector meson exchange. For σ exchange,

$$\mathcal{V}_{\sigma}^{[J]}(\mathbf{q}) = -g_{\sigma}^2 \mathcal{C}[J] \frac{1}{\mathbf{q}^2 + m_{\sigma}^2} \quad (23)$$

with

$$\begin{aligned} \mathcal{A}[J] & \equiv \sum_{\lambda_1\lambda_2\lambda_3\lambda_4} \langle 1\lambda_1; 1\lambda_2 | J, m \rangle \langle 1\lambda_3; 1\lambda_4 | J, m \rangle \frac{1}{\mathbf{q}^2} \\ & \times [\epsilon_1^{\lambda_1} \cdot (\mathbf{q} \times \epsilon_3^{*\lambda_3}) \epsilon_2^{\lambda_2} \cdot (\mathbf{q} \times \epsilon_4^{*\lambda_4})], \end{aligned} \quad (24)$$

$$\begin{aligned} \mathcal{B}[J] & \equiv \sum_{\lambda_1\lambda_2\lambda_3\lambda_4} \langle 1\lambda_1; 1\lambda_2 | J, m \rangle \langle 1\lambda_3; 1\lambda_4 | J, m \rangle \frac{1}{\mathbf{q}^2} \\ & \times [(\epsilon_1 \cdot \mathbf{q})(\epsilon_2 \cdot \mathbf{q})(\epsilon_3^* \cdot \epsilon_4^*) + (\text{c.t.s})], \end{aligned} \quad (25)$$

$$\begin{aligned} \mathcal{C}[J] & \equiv \sum_{\lambda_1\lambda_2\lambda_3\lambda_4} \langle 1\lambda_1; 1\lambda_2 | J, m \rangle \langle 1\lambda_3; 1\lambda_4 | J, m \rangle \\ & \times (\epsilon_1^{\lambda_1} \cdot \epsilon_3^{*\lambda_3})(\epsilon_2^{\lambda_2} \cdot \epsilon_4^{*\lambda_4}), \end{aligned} \quad (26)$$

where ϵ_i is the polarization vector, and c.t.s denotes the cross-terms, i.e. $-(\epsilon_1 \cdot \mathbf{q})(\epsilon_4^* \cdot \mathbf{q})(\epsilon_2 \cdot \epsilon_3^*)$, $(\epsilon_3^* \cdot \mathbf{q})(\epsilon_4^* \cdot \mathbf{q}) \times (\epsilon_1 \cdot \epsilon_2)$ and $-(\epsilon_3^* \cdot \mathbf{q})(\epsilon_2 \cdot \mathbf{q})(\epsilon_1 \cdot \epsilon_4^*)$. When considering the different systems with $J^P = 0^+, 1^+, 2^+$, we impose the constraint on the scattering amplitudes that the initial states and final states should have the same angular momentum. Then we average the potential in the momentum space, i.e., making the substitutions $q_{x,y,z}^2 \rightarrow q^2/3$. The coefficients of $\mathcal{A}(J)$, $\mathcal{B}(J)$ and $\mathcal{C}(J)$ are listed into Table 4.

After Fourier transformation, we get the potentials in the coordinate space

$$\begin{aligned} \mathcal{V}_{\mathbb{P}}^{[J]}(r) & [I_1^{\mathbb{P}\mathcal{D}_1^*\mathcal{D}_1^*}, I_2^{\mathbb{P}\mathcal{D}_2^*\mathcal{D}_2^*}, m_{\mathcal{D}_1^*}, m_{\mathcal{D}_2^*}, m_{\mathbb{P}}] \\ & = \frac{1}{4} g_{\mathcal{D}^*\mathcal{D}^*\mathbb{P}}^2 I_1^{\mathbb{P}\mathcal{D}_1^*\mathcal{D}_1^*} I_2^{\mathbb{P}\mathcal{D}_2^*\mathcal{D}_2^*} \mathcal{A}[J] Z[\Lambda, m_{\mathbb{P}}, r], \end{aligned} \quad (27)$$

Table 4 The values of $\mathcal{A}(J)$, $\mathcal{B}(J)$ and $\mathcal{C}(J)$ for the cases of the $J^P = 0^+, 1^+, 2^+$ systems

J	$\mathcal{A}(J)$	$\mathcal{B}(J)$	$\mathcal{C}(J)$
0	2/3	4/3	1
1	1/3	2/3	1
2	-1/3	-2/3	1

$$\begin{aligned} \mathcal{V}_{\mathbb{V}}^{[J]}(r) & [I_1^{\mathbb{V}\mathcal{D}_1^*\mathcal{D}_1^*}, I_2^{\mathbb{V}\mathcal{D}_2^*\mathcal{D}_2^*}, m_{\mathcal{D}_1^*}, m_{\mathcal{D}_2^*}, m_{\mathbb{V}}] \\ & = -I_1^{\mathbb{V}\mathcal{D}_1^*\mathcal{D}_1^*} I_2^{\mathbb{V}\mathcal{D}_2^*\mathcal{D}_2^*} \left[\frac{g_{\mathcal{D}^*\mathcal{D}^*\mathbb{V}}^2}{4m_{\mathcal{D}_1^*}^2 m_{\mathcal{D}_2^*}^2} \mathcal{C}[J] \frac{1}{m_{\mathbb{V}}^2} X[\Lambda, m_{\mathbb{V}}, r] \right. \\ & \quad + g_{\mathcal{D}^*\mathcal{D}^*\mathbb{V}}^2 \mathcal{C}[J] Y[\Lambda, m_{\mathbb{V}}, r] \\ & \quad \left. + \frac{4f_{\mathcal{D}^*\mathcal{D}^*\mathbb{V}}^2}{m_{\mathcal{D}_1^*}^2 m_{\mathcal{D}_2^*}^2} \mathcal{B}[J] Z[\Lambda, m_{\mathbb{V}}, r] \right], \end{aligned} \quad (28)$$

$$\mathcal{V}_\sigma(r)^{[J]} = -g_\sigma^2 \mathcal{C}[J] Y[\Lambda, m_\sigma, r]. \quad (29)$$

The total effective potentials for the $\Phi_s^{**\pm}$ and $\Phi_s^0(\bar{\Phi}_s^0)$ states are

$$\mathcal{V}(r)_{\text{Total}}^{\Phi_s^\pm[J]} = \mathcal{V}_{\mathbb{P}}^{[J]}(r) \left[\frac{1}{\sqrt{6}}, -\frac{2}{\sqrt{6}}, m_{D^{*0}}, m_{D_s^*}, m_\eta \right], \quad (30)$$

$$\begin{aligned} \mathcal{V}(r)_{\text{Total}}^{\Phi_s^0(\bar{\Phi}_s^0)[J]} & = \mathcal{V}_{\mathbb{P}}^{[J]}(r) \left[\frac{1}{\sqrt{6}}, -\frac{2}{\sqrt{6}}, m_{D^{*+}}, m_{D_s^*}, m_\eta \right], \end{aligned} \quad (31)$$

where only η meson exchange is allowed. Considering the SU(2) symmetry, one further gets

$$\begin{aligned} \mathcal{V}(r)_{\text{Total}}^{\Phi_s^\pm[J]} & \approx \mathcal{V}(r)_{\text{Total}}^{\Phi_s^0(\bar{\Phi}_s^0)[J]} \\ & = -\frac{1}{12} g_{\mathcal{D}^*\mathcal{D}^*\mathbb{P}}^2 \mathcal{A}[J] Z[\Lambda, m_\eta, r]. \end{aligned} \quad (32)$$

For the Φ_{s1}^{**0} state, the potential is

$$\begin{aligned} \mathcal{V}(r)_{\text{Total}}^{\Phi_{s1}^{**0}[J]} & = \mathcal{V}_{\mathbb{P}}^{[J]}(r) \left[-\frac{2}{\sqrt{6}}, -\frac{2}{\sqrt{6}}, m_{D_s^*}, m_{D_s^*}, m_\eta \right] \\ & \quad + \mathcal{V}_{\mathbb{V}}^{[J]}(r) [1, 1, m_{D_s^*}, m_{D_s^*}, m_\phi] \\ & = \frac{1}{6} g_{\mathcal{D}^*\mathcal{D}^*\mathbb{P}}^2 \mathcal{A}[J] Z[\Lambda, m_\eta, r] \\ & \quad - \left[\frac{g_{\mathcal{D}^*\mathcal{D}^*\mathbb{V}}^2}{4m_{\mathcal{D}_s^*}^2 m_\phi^2} \mathcal{C}[J] X[\Lambda, m_\phi, r] \right. \\ & \quad + g_{\mathcal{D}^*\mathcal{D}^*\mathbb{V}}^2 \mathcal{C}[J] Y[\Lambda, m_\phi, r] \\ & \quad \left. + \frac{4f_{\mathcal{D}^*\mathcal{D}^*\mathbb{V}}^2}{m_{\mathcal{D}_s^*}^2} \mathcal{B}[J] Z[\Lambda, m_\phi, r] \right]. \end{aligned} \quad (33)$$

For $\Phi^{**\pm}$, the exchange potential reads

$$\begin{aligned} \mathcal{V}(r)_{\text{Total}}^{\Phi^{**\pm}[J]} & = \mathcal{V}_{\mathbb{P}}^{[J]}(r) \left[\frac{1}{\sqrt{2}}, -\frac{1}{\sqrt{2}}, m_{D^{*0}}, m_{D^{*+}}, m_\pi \right] \\ & \quad + \mathcal{V}_{\mathbb{P}}^{[J]}(r) \left[\frac{1}{\sqrt{6}}, \frac{1}{\sqrt{6}}, m_{D^{*0}}, m_{D^{*+}}, m_\eta \right] \\ & \quad + \mathcal{V}_{\mathbb{V}}^{[J]}(r) \left[\frac{1}{\sqrt{2}}, -\frac{1}{\sqrt{2}}, m_{D^{*0}}, m_{D^{*+}}, m_\rho \right] \\ & \quad + \mathcal{V}_{\mathbb{V}}^{[J]}(r) \left[\frac{1}{\sqrt{2}}, \frac{1}{\sqrt{2}}, m_{D^{*0}}, m_{D^{*+}}, m_\omega \right] \\ & \quad + \mathcal{V}_\sigma(r)^{[J]} \\ & \approx -g_{\mathcal{D}^*\mathcal{D}^*\mathbb{P}}^2 \mathcal{A}[J] \left[\frac{Z[\Lambda, m_\pi, r]}{8} \right. \\ & \quad \left. - \frac{Z[\Lambda, m_\eta, r]}{24} \right] - g_\sigma^2 \mathcal{C}[J] Y[\Lambda, m_\sigma, r] \\ & \quad + \frac{1}{2} \left[\frac{g_{\mathcal{D}^*\mathcal{D}^*\mathbb{V}}^2}{4m_{\mathcal{D}^*}^2 m_\rho^2} \mathcal{C}[J] X[\Lambda, m_\rho, r] \right. \\ & \quad + g_{\mathcal{D}^*\mathcal{D}^*\mathbb{V}}^2 \mathcal{C}[J] Y[\Lambda, m_\rho, r] \\ & \quad \left. + \frac{4f_{\mathcal{D}^*\mathcal{D}^*\mathbb{V}}^2}{m_{\mathcal{D}^*}^2} \mathcal{B}[J] Z[\Lambda, m_\rho, r] \right] \\ & \quad - \frac{1}{2} \left[\frac{g_{\mathcal{D}^*\mathcal{D}^*\mathbb{V}}^2}{4m_{\mathcal{D}^*}^2 m_\omega^2} \mathcal{C}[J] X[\Lambda, m_\omega, r] \right. \\ & \quad + g_{\mathcal{D}^*\mathcal{D}^*\mathbb{V}}^2 \mathcal{C}[J] Y[\Lambda, m_\omega, r] \\ & \quad \left. + \frac{4f_{\mathcal{D}^*\mathcal{D}^*\mathbb{V}}^2}{m_{\mathcal{D}^*}^2} \mathcal{B}[J] Z[\Lambda, m_\omega, r] \right]. \end{aligned} \quad (34)$$

The potential for the $\Phi^{**0}(\Phi_8^{**0})$ state is

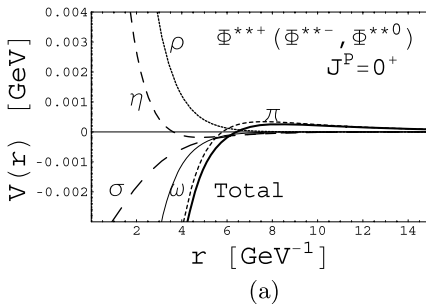
$$\begin{aligned} \mathcal{V}(r)_{\text{Total}}^{\Phi^{**0}(\Phi_8^{**0})[J]} & = \frac{1}{2} \left\{ \mathcal{V}_{\mathbb{P}}^{[J]}(r) \left[\frac{1}{\sqrt{2}}, \frac{1}{\sqrt{2}}, m_{D^{*0}}, m_{D^{*0}}, m_{\pi^0} \right] \right. \\ & \quad \mp 2\mathcal{V}_{\mathbb{P}}^{[J]}(r) [1, 1, m_{D^{*0}}, m_{D^{*+}}, m_{\pi^\pm}] \\ & \quad + \mathcal{V}_{\mathbb{P}}^{[J]}(r) \left[-\frac{1}{\sqrt{2}}, -\frac{1}{\sqrt{2}}, m_{D^{*+}}, m_{D^{*-}}, m_{\pi^0} \right] \\ & \quad + \mathcal{V}_{\mathbb{P}}^{[J]}(r) \left[\frac{1}{\sqrt{6}}, \frac{1}{\sqrt{6}}, m_{D^{*0}}, m_{D^{*0}}, m_\eta \right] \\ & \quad + \mathcal{V}_{\mathbb{P}}^{[J]}(r) \left[\frac{1}{\sqrt{6}}, \frac{1}{\sqrt{6}}, m_{D^{*+}}, m_{D^{*-}}, m_\eta \right] \\ & \quad + \mathcal{V}_{\mathbb{V}}^{[J]}(r) \left[\frac{1}{\sqrt{2}}, \frac{1}{\sqrt{2}}, m_{D^{*0}}, m_{D^{*0}}, m_{\rho^0} \right] \\ & \quad \mp 2\mathcal{V}_{\mathbb{V}}^{[J]}(r) [1, 1, m_{D^{*0}}, m_{D^{*+}}, m_{\rho^\pm}] \\ & \quad + \mathcal{V}_{\mathbb{V}}^{[J]}(r) \left[-\frac{1}{\sqrt{2}}, -\frac{1}{\sqrt{2}}, m_{D^{*+}}, m_{D^{*-}}, m_{\rho^0} \right] \end{aligned}$$

$$\begin{aligned}
& + \mathcal{V}_{\bar{V}}^{[J]}(r) \left[\frac{1}{\sqrt{2}}, \frac{1}{\sqrt{2}}, m_{D^{*0}}, m_{D^{*0}}, m_{\omega} \right] \\
& + \mathcal{V}_{\bar{V}}^{[J]}(r) \left[\frac{1}{\sqrt{2}}, \frac{1}{\sqrt{2}}, m_{D^{*+}}, m_{D^{*-}}, m_{\omega} \right] + 2\mathcal{V}_{\sigma}^{[J]}(r) \Big\} \\
& \approx g_{D^* D^* \bar{V}}^2 \mathcal{A}[J] \left[\frac{(1 \mp 2)}{8} Z[\Lambda, m_{\pi}, r] + \frac{Z[\Lambda, m_{\eta}, r]}{24} \right] \\
& - g_{\sigma}^2 \mathcal{C}[J] Y[\Lambda, m_{\sigma}, r] \\
& - \frac{(1 \mp 2)}{2} \left[\frac{g_{D^* D^* \bar{V}}^2}{4m_{D^*}^2 m_{\rho}^2} \mathcal{C}[J] X[\Lambda, m_{\rho}, r] \right. \\
& + g_{D^* D^* \bar{V}}^2 \mathcal{C}[J] Y[\Lambda, m_{\rho}, r] \\
& \left. + \frac{4f_{D^* D^* \bar{V}}^2}{m_{D^*}^2} \mathcal{B}[J] Z[\Lambda, m_{\rho}, r] \right] \\
& - \frac{1}{2} \left[\frac{g_{D^* D^* \bar{V}}^2}{4m_{D^*}^2 m_{\omega}^2} \mathcal{C}[J] X[\Lambda, m_{\omega}, r] \right. \\
& + g_{D^* D^* \bar{V}}^2 \mathcal{C}[J] Y[\Lambda, m_{\omega}, r] \\
& \left. + \frac{4f_{D^* D^* \bar{V}}^2}{m_{D^*}^2} \mathcal{B}[J] Z[\Lambda, m_{\omega}, r] \right], \quad (35)
\end{aligned}$$

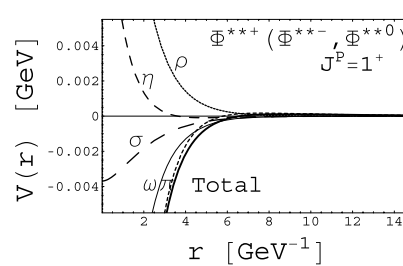
where \mp corresponds to $\Phi^{**0}(\Phi_s^{**0})$ respectively. As a cross-check, the potential for Φ^{**0} is the same as that for $\Phi^{**\pm}$ by SU(2) symmetry. For the V–V systems, we need only consider four independent types of potentials corresponding to $[\Phi_s^{**\pm}, \Phi_s^{**0}, \bar{\Phi}_s^{**0}]$, $[\Phi^{**\pm}, \Phi^{**0}]$, Φ_8^{**0} and Φ_{s1}^{**0} listed in (32), (34), (35), (33) respectively when we consider the SU(2) symmetry. For states with different quantum numbers, we simply change the values of $\mathcal{A}[J]$, $\mathcal{B}[J]$ and $\mathcal{C}[J]$ in Table 4.

5.2 Numerical results for the V–V system

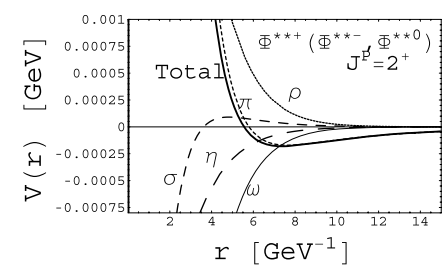
The quantum numbers of the S-wave V–V system are $J^P = 0^+, 1^+, 2^+$. The variation of the oscillating effective potential of $\Phi_s^{**\pm}(\Phi_s^{**0}, \bar{\Phi}_s^{**0})$ with r is shown in Fig. 4, where



(a)



(b)



(c)

Fig. 5 The effective potentials of $\Phi^{**\pm}(\Phi^{**0})$ with different quantum numbers. The thick solid line is the total effective potential. Here we take the cutoff $\Lambda = 1$ GeV

only η meson exchange is allowed. The effective potentials of $\Phi^{*\pm}(\Phi^{*0})$ and Φ_8^{**0} with $J^P = 0^+, 1^+, 2^+$ are presented in Figs. 5–6, where the exchanged mesons include π , η , ρ , ω and σ . For Φ_{s1}^{**0} , its effective potential is shown in Fig. 7, where both η and ϕ meson exchange is allowed.

With the above effective potentials, we solve the Schrödinger equation to find the bound state solutions for the V–V system. Numerical results are collected in Fig. 8 and Tables 5–7. For the $D^* - \bar{D}^*$ states with $J^P = 0^+, 1^+$, a bound state exists only for Λ much larger than 1 GeV. Especially for $\Phi_s^{**\pm}(\Phi_s^{**0}, \bar{\Phi}_s^{**0})$ and $\Phi^{**\pm}(\Phi^{**0})$ with $J^P = 1^+$, the existence of a bound state requires the values of Λ be larger than 8 GeV. For $\Phi_s^{**\pm}(\Phi_s^{**0}, \bar{\Phi}_s^{**0})$ and $\Phi^{**\pm}(\Phi^{**0})$ with $J^P = 2^+$, no bound states exists for $\Lambda < 10$ GeV. The cut-off parameter Λ is a typical hadronic scale, which is generally expected to be around 1–2 GeV. If Λ is much larger than 2 GeV or much smaller than 1 GeV in order to form a bound state, we tend to conclude that there does not exist a heavy molecular state for these systems. We find bound state solutions for Φ_8^{**0} and Φ_{s1}^{**0} with $J^P = 0^+, 1^+, 2^+$.

There do not exist molecular states $\Omega_s^{**\pm}(\Omega_s^{**0}, \bar{\Omega}_s^{**0})$ and $\Omega^{**\pm}(\Omega^{**0})$ with $J^P = 2^+$ since we can not find bound state solutions for $\Lambda = 0$ –10 GeV. Different from the $D^* - \bar{D}^*$ system, there exist possible molecular states

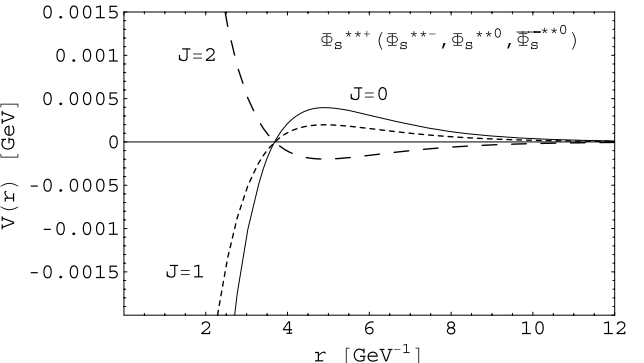


Fig. 4 The effective potential of $\Phi_s^{**\pm}(\Phi_s^{**0}, \bar{\Phi}_s^{**0})$ with the cutoff $\Lambda = 1$ GeV

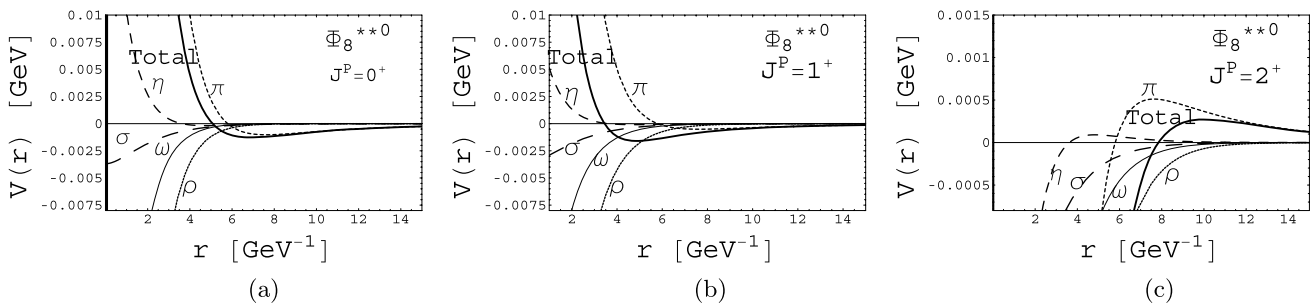


Fig. 6 The shape of the exchange potential of Φ_8^{**0} . The thick solid line is the total effective potential. Here we take the cutoff $\Lambda = 1$ GeV

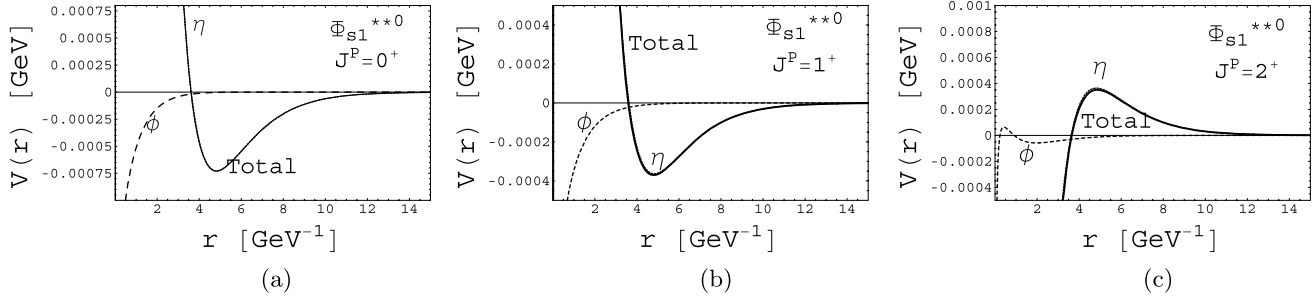


Fig. 7 The variation of the effective potential of Φ_{s1}^{**0} with r . The thick solid line is the total effective potential. Here we take the cutoff $\Lambda = 1$ GeV

$\Omega_s^{**\pm}(\Omega_s^{**0}, \bar{\Omega}_s^{**0})$ with $J^P = 0^+, 1^+$ with more reasonable Λ close to 1 GeV. We also find the bound state solutions for Ω_8^{**0} and Ω_{s1}^{**0} . The reason is simple. The larger the reduced mass for $B^* - \bar{B}^*$, the lower the kinetic energy, the easier to form a molecular state. With Φ_s^{**} as an example, we illustrate the dependence of E on Λ in Fig. 8.

6 The $\mathcal{D}^* - \bar{\mathcal{D}}$ case

6.1 The potential of the P–V system

Figure 9 shows the general scattering channels in the derivation of the exchange potential. Different from the P–P and V–V systems, we need consider two additional crossed scattering diagrams for the P–V system, i.e. Fig. 9(b) and (c).

In terms of the effective Lagrangian in Sect. 3, the σ meson exchange potential in the momentum space is¹

$$\mathcal{V}_\sigma(\mathbf{q}) = -\frac{g_\sigma^2}{\mathbf{q}^2 + m_\sigma^2}. \quad (36)$$

The pseudoscalar meson exchange potential reads [17, 18]

$$\begin{aligned} \mathcal{V}_{\mathbb{P}}(\mathbf{q}) & [I_1^{\mathbb{P}\mathcal{D}_1\mathcal{D}_2^*}, I_2^{\mathbb{P}\mathcal{D}_2^*\mathcal{D}_1}, m_{\mathcal{D}_1}, m_{\mathcal{D}_2^*}, m_{\mathbb{P}}] \\ &= -\frac{1}{12m_{\mathcal{D}_1}m_{\mathcal{D}_2^*}} g_{\mathcal{D}^*\mathcal{D}\mathbb{P}}^2 I_1^{\mathbb{P}\mathcal{D}_1\mathcal{D}_2^*} I_2^{\mathbb{P}\mathcal{D}_2^*\mathcal{D}_1} \\ &\times \begin{cases} \frac{\mathbf{q}^2}{\mu^2 - \mathbf{q}^2} & \text{for } \pi, \\ -\frac{\mathbf{q}^2}{\mathbf{q}^2 + \mu^2} & \text{for } \eta, \end{cases} \end{aligned} \quad (37)$$

where $\mu = \sqrt{q_0^2 - m_\pi^2}$, $\mu' = \sqrt{m_{\eta(K)}^2 - q_0^2}$ and $q_0 = m_{\mathcal{D}_2^*} - m_{\mathcal{D}_1}$. For vector meson exchange, there exist two types of potentials from the direct and crossed scattering channels:

$$\begin{aligned} \mathcal{V}_{\mathbb{V}}^{\text{Direct}}(\mathbf{q}) & [I_1^{\mathbb{V}\mathcal{D}_1\mathcal{D}_1}, I_2^{\mathbb{V}\mathcal{D}_2^*\mathcal{D}_2^*}, m_{\mathcal{D}_1}, m_{\mathcal{D}_2^*}, m_{\mathbb{V}}] \\ &= -g_{\mathcal{D}\mathcal{D}\mathbb{V}} g_{\mathcal{D}^*\mathcal{D}^*\mathbb{V}} I_1^{\mathbb{V}\mathcal{D}_1\mathcal{D}_1} I_2^{\mathbb{V}\mathcal{D}_2^*\mathcal{D}_2^*} \\ &\times \left(\frac{\mathbf{q}^2}{4m_{\mathcal{D}_1}m_{\mathcal{D}_2^*}m_{\mathbb{V}}^2} + \frac{1}{\mathbf{q}^2 + m_{\mathbb{V}}^2} \right), \end{aligned} \quad (38)$$

$$\begin{aligned} \mathcal{V}_{\mathbb{V}}^{\text{Cross}}(\mathbf{q}) & [I_1^{\mathbb{V}\mathcal{D}_1\mathcal{D}_2^*}, I_2^{\mathbb{V}\mathcal{D}_2^*\mathcal{D}_1}, m_{\mathcal{D}_1}, m_{\mathcal{D}_2^*}, m_{\mathbb{V}}] \\ &= -\frac{8}{3} f_{\mathcal{D}^*\mathcal{D}\mathbb{V}}^2 I_1^{\mathbb{V}\mathcal{D}_1\mathcal{D}_2^*} I_2^{\mathbb{V}\mathcal{D}_2^*\mathcal{D}_1} \frac{\mathbf{q}^2}{\mathbf{q}^2 + \zeta^2}, \end{aligned} \quad (39)$$

¹We missed a minus sign in the sigma meson exchange potential in [17, 18].

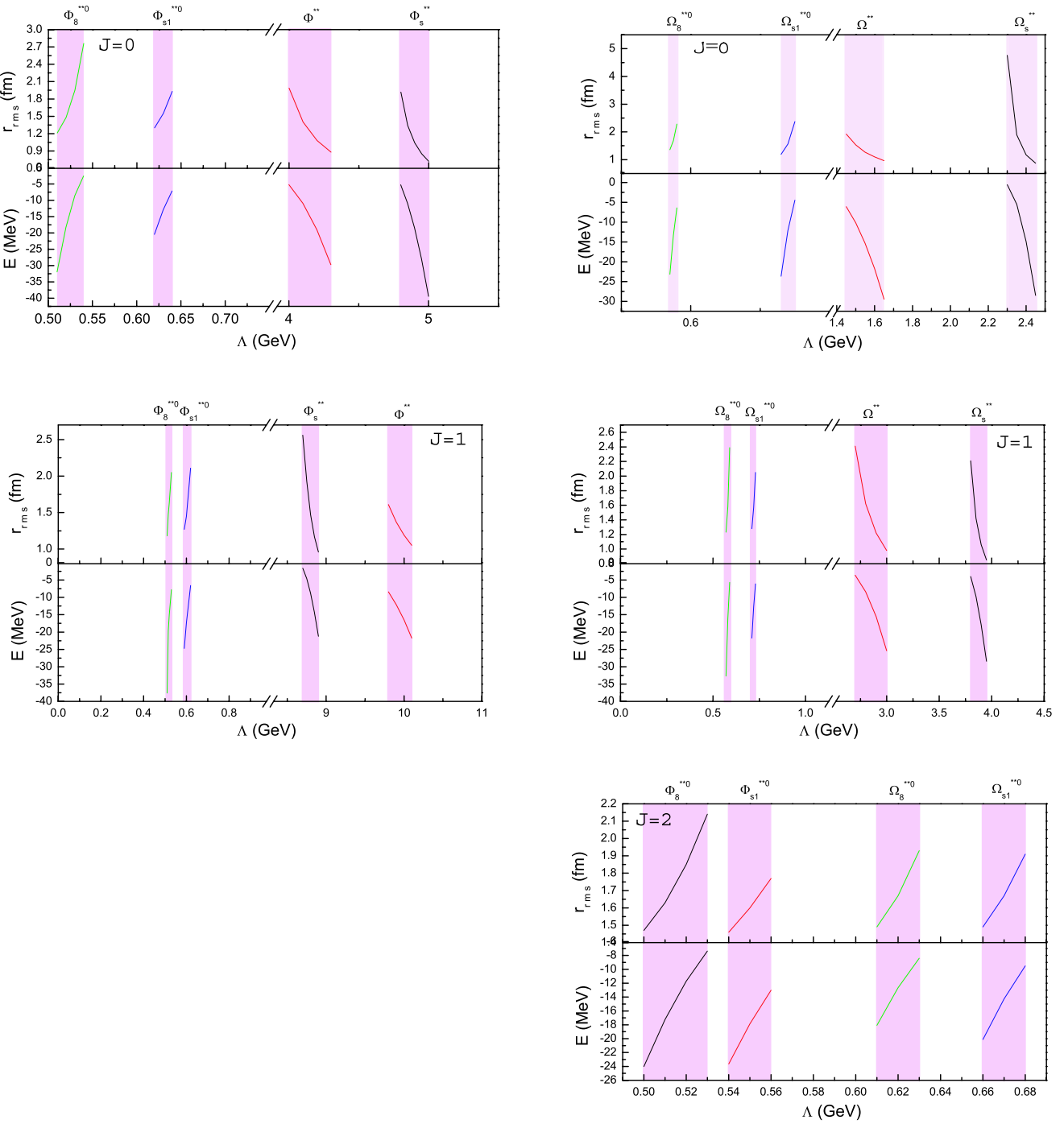


Fig. 8 The dependence of binding energy E and r_{rms} on Λ for the V–V system

where $\zeta_V = \sqrt{m_V^2 - q_0^2}$. One notes that m_V is larger than q_0 for the P–V case. After Fourier transformation, we obtain the effective potentials in the coordinate space

$$\mathcal{V}_\sigma(r) = -g_\sigma^2 Y[\Lambda, m_\sigma, r], \quad (40)$$

$$\begin{aligned} \mathcal{V}_{\mathbb{P}}(r) & [I_1^{\mathbb{P}\mathcal{D}_1\mathcal{D}_2^*}, I_2^{\mathbb{P}\mathcal{D}_2^*\mathcal{D}_1}, m_{\mathcal{D}_1}, m_{\mathcal{D}_2^*}, m_{\mathbb{P}}] \\ & = -\frac{1}{12m_{\mathcal{D}_1}m_{\mathcal{D}_2^*}} g_{\mathcal{D}^*\mathcal{D}\mathbb{P}}^2 I_1^{\mathbb{P}\mathcal{D}_1\mathcal{D}_2^*} I_2^{\mathbb{P}\mathcal{D}_2^*\mathcal{D}_1} \\ & \times \begin{cases} U(r) & \text{for } \pi, \\ -Z[\Lambda, \mu', r] & \text{for } \eta, \end{cases} \end{aligned} \quad (41)$$

Table 5 The numerical results for the $\mathcal{D}^* - \bar{\mathcal{D}}^*$ and $\mathcal{B}^* - \bar{\mathcal{B}}^*$ systems

State	$\mathcal{D}^* - \bar{\mathcal{D}}^*$								
	$J^P = 0^+$			$J^P = 1^+$			$J^P = 2^+$		
	Λ (GeV)	E (MeV)	r_{rms} (fm)	Λ (GeV)	E (MeV)	r_{rms} (fm)	Λ (GeV)	E (MeV)	r_{rms} (fm)
$\Phi_s^{**\pm}(\Phi_s^{**0}, \bar{\Phi}_s^{**0})$	4.80	-5.26	1.92	8.70	-1.60	2.56	-	-	-
	4.85	-10.90	1.34	8.75	-4.59	1.93	-	-	-
	4.90	-18.49	1.04	8.80	-8.83	1.47	-	-	-
	4.95	-27.99	0.85	8.85	-14.36	1.17	-	-	-
	5.00	-39.42	0.72	8.90	-21.21	0.96	-	-	-
$\Phi^{**\pm}(\Phi^{**0})$	4.00	-5.21	1.99	9.80	-8.40	1.61	-	-	-
	4.10	-10.93	1.40	9.90	-12.08	1.37	-	-	-
	4.20	-19.02	1.08	10.00	-16.53	1.19	-	-	-
	4.30	-29.73	0.88	10.10	-21.75	1.05	-	-	-
Φ_8^{**0}	0.51	-31.92	1.21	0.51	-37.61	1.18	0.50	-24.01	1.47
	0.52	-18.32	1.48	0.515	-19.63	1.48	0.51	-17.23	1.63
	0.53	-8.61	1.95	0.52	-15.03	1.63	0.52	-11.71	1.85
	0.54	-2.57	2.76	0.53	-7.77	2.05	0.53	-7.36	2.14
Φ_{s1}^{**0}	0.62	-20.46	1.30	0.59	-24.74	1.27	0.54	-23.64	1.46
	0.63	-12.91	1.55	0.60	-17.27	1.45	0.55	-17.87	1.60
	0.64	-7.13	1.93	0.62	-6.56	2.11	0.56	-13.01	1.77
State	$\mathcal{B}^* - \bar{\mathcal{B}}^*$								
	$J^P = 0^+$			$J^P = 1^+$			$J^P = 2^+$		
	Λ (GeV)	E (MeV)	r_{rms} (fm)	Λ (GeV)	E (MeV)	r_{rms} (fm)	Λ (GeV)	E (MeV)	r_{rms} (fm)
$\Omega_s^{**\pm}(\Omega_s^{**0}, \bar{\Omega}_s^{**0})$	2.30	-0.57	4.76	3.80	-3.98	2.21	-	-	-
	2.35	-5.52	1.89	3.85	-9.75	1.42	-	-	-
	2.40	-14.90	1.17	3.90	-17.91	1.06	-	-	-
	2.45	-28.50	0.87	3.95	-28.43	0.85	-	-	-
$\Omega^{**\pm}(\Omega^{**0})$	1.45	-6.12	1.92	-	-	-	-	-	-
	1.50	-10.17	1.53	2.70	-3.60	2.41	-	-	-
	1.55	-15.35	1.27	2.80	-8.40	1.62	-	-	-
	1.60	-21.75	1.10	2.90	-15.55	1.22	-	-	-
	1.65	-29.46	0.96	3.00	-25.38	0.98	-	-	-
Ω_8^{**0}	0.57	-23.16	1.36	0.57	-32.70	1.23	0.61	-18.07	1.49
	0.575	-13.34	1.68	0.58	-16.11	1.58	0.62	-12.66	1.67
	0.58	-6.42	2.28	0.59	-5.65	2.39	0.63	-8.39	1.93
Ω_{s1}^{**0}	0.73	-23.67	1.19	0.71	-21.76	1.28	0.66	-20.11	1.49
	0.74	-12.12	1.56	0.72	-12.68	1.57	0.67	-14.26	1.67
	0.75	-4.48	2.37	0.73	-6.12	2.05	0.68	-9.50	1.91

$$\begin{aligned} & \mathcal{V}_{\mathbb{V}}^{\text{Direct}}(r) [I_1^{\mathbb{V}\mathcal{D}_1\mathcal{D}_1}, I_2^{\mathbb{V}\mathcal{D}_2^*\mathcal{D}_2^*}, m_{\mathcal{D}_1}, m_{\mathcal{D}_2^*}, m_{\mathbb{V}}] \\ &= -g_{\mathcal{D}\mathcal{D}\mathbb{V}} g_{\mathcal{D}^*\mathcal{D}^*\mathbb{V}} I_1^{\mathbb{V}\mathcal{D}_1\mathcal{D}_1} I_2^{\mathbb{V}\mathcal{D}_2^*\mathcal{D}_2^*} \\ & \quad \times \left(\frac{X[\Lambda, m_{\mathbb{V}}, r]}{4m_{\mathcal{D}_1}m_{\mathcal{D}_2^*}m_{\mathbb{V}}^2} + Y[\Lambda, m_{\mathbb{V}}, r] \right), \end{aligned} \quad (42)$$

$$\begin{aligned} & \mathcal{V}_{\mathbb{V}}^{\text{Cross}}(r) [I_1^{\mathbb{V}\mathcal{D}_1\mathcal{D}_2^*}, I_2^{\mathbb{V}\mathcal{D}_2^*\mathcal{D}_1}, m_{\mathcal{D}_1}, m_{\mathcal{D}_2^*}, m_{\mathbb{V}}] \\ &= -\frac{8}{3} f_{\mathcal{D}^*\mathcal{D}\mathbb{V}}^2 I_1^{\mathbb{V}\mathcal{D}_1\mathcal{D}_2^*} I_2^{\mathbb{V}\mathcal{D}_2^*\mathcal{D}_1} Z[\Lambda, \xi_{\mathbb{V}}, r]. \end{aligned} \quad (43)$$

Table 6 The numerical results for the $\mathcal{D}^* - \bar{\mathcal{D}}^*$ and $\mathcal{B}^* - \bar{\mathcal{B}}^*$ systems after increasing the coupling constants by a factor of two

State	$\mathcal{D}^* - \bar{\mathcal{D}}^*$								
	$J^P = 0^+$			$J^P = 1^+$			$J^P = 2^+$		
	Λ (GeV)	E (MeV)	r_{rms} (fm)	Λ (GeV)	E (MeV)	r_{rms} (fm)	Λ (GeV)	E (MeV)	r_{rms} (fm)
$\Phi_s^{*\pm}(\Phi_s^{*0}, \bar{\Phi}_s^{*0})$	1.90	-16.07	1.14	2.90	-14.48	1.18	-	-	-
	1.85	-4.7	2.05	2.80	-1.14	3.74	-	-	-
$\Phi^{*\pm}(\Phi^{*0})$	1.00	-5.42	2.06	1.80	-6.28	1.89	-	-	-
	1.20	-36.75	0.92	2.00	-24.25	1.04	-	-	-
Φ_8^{*0}	0.58	-45.86	1.05	0.60	-15.53	1.62	0.65	-32.94	1.15
	0.59	-13.02	1.73	0.61	-3.64	2.64	0.66	-27.10	1.21
Φ_{s1}^{*0}	0.76	-39.20	0.97	0.74	-38.98	1.01	0.70	-23.96	1.38
	0.78	-7.90	1.82	0.76	-12.73	1.55	0.72	-11.31	1.78
State	$\mathcal{B}^* - \bar{\mathcal{B}}^*$								
	$J^P = 0^+$			$J^P = 1^+$			$J^P = 2^+$		
	Λ (GeV)	E (MeV)	r_{rms} (fm)	Λ (GeV)	E (MeV)	r_{rms} (fm)	Λ (GeV)	E (MeV)	r_{rms} (fm)
$\mathcal{Q}_s^{*\pm}(\mathcal{Q}_s^{*0}, \bar{\mathcal{Q}}_s^{*0})$	1.20	-9.26	1.50	1.60	-6.27	1.79	-	-	-
	1.30	-79.29	0.60	1.70	-44.38	0.73	-	-	-
$\mathcal{Q}^{*\pm}(\mathcal{Q}^{*0})$	0.50	-17.96	1.41	0.80	-7.74	1.80	-	-	-
	0.48	-16.36	1.48	0.90	-25.86	1.11	-	-	-
\mathcal{Q}_8^{*0}	0.60	-81.06	0.89	0.62	-46.66	1.15	0.70	-245.16	0.50
	0.61	-10.73	2.15	0.63	-11.49	1.98	0.71	-352.21	0.49
\mathcal{Q}_{s1}^{*0}	0.83	-25.32	1.17	0.82	-34.93	1.06	0.80	-26.93	1.27
	0.84	-5.08	2.18	0.83	-15.01	1.47	0.82	-11.66	1.69

Here

$$U(r) = -\frac{\mu^2}{4\pi r} [\cos(\mu r) - e^{-\alpha r}] - \frac{\beta^2 \alpha}{8\pi} e^{-\alpha r}$$

with $\beta = \sqrt{\Lambda^2 - m_\pi^2}$ and $\alpha = \sqrt{\Lambda^2 - q_0^2}$. The total effective potentials of $\Phi_s^{*\pm}/\hat{\Phi}_s^{*\pm}$, $\Phi_s^{*0}/\hat{\Phi}_s^{*0}$, $\bar{\Phi}_s^{*0}/\hat{\bar{\Phi}}_s^{*0}$ are

$$\mathcal{V}(r)_{\text{Total}}^{\Phi_s^{*\pm}/\hat{\Phi}_s^{*\pm}} = c \frac{g_{\mathcal{D}^*\mathcal{D}\mathbb{P}}^2}{36\sqrt{m_D m_{D_s} m_{D^*} m_{D_s^*}}} Z[\Lambda, \mu', r]. \quad (44)$$

For $\Phi^{*\pm}/\hat{\Phi}^{*\pm}$, the total effective potential reads

$$\begin{aligned} \mathcal{V}(r)_{\text{Total}}^{\Phi^{*\pm}/\hat{\Phi}^{*\pm}} &= \frac{1}{2} g_{\mathcal{D}\mathcal{D}\mathbb{V}} g_{\mathcal{D}^*\mathcal{D}^*\mathbb{V}} \left[\frac{X[\Lambda, m_\rho, r]}{4m_D m_{D^*} m_\rho^2} + Y[\Lambda, m_\rho, r] \right] \\ &\quad - \frac{1}{2} g_{\mathcal{D}\mathcal{D}\mathbb{V}} g_{\mathcal{D}^*\mathcal{D}^*\mathbb{V}} \left[\frac{X[\Lambda, m_\omega, r]}{4m_D m_{D^*} m_\omega^2} + Y[\Lambda, m_\omega, r] \right] \\ &\quad - c \left\{ -\frac{g_{\mathcal{D}^*\mathcal{D}\mathbb{P}}^2}{24m_D m_{D^*}} U(r) - \frac{g_{\mathcal{D}^*\mathcal{D}\mathbb{P}}^2}{72m_D m_{D^*}} Z[\Lambda, \mu', r] \right. \\ &\quad \left. - \frac{4}{3} f_{\mathcal{D}^*\mathcal{D}\mathbb{V}}^2 Z[\Lambda, \zeta_\rho, r] + \frac{4}{3} f_{\mathcal{D}^*\mathcal{D}\mathbb{V}}^2 Z[\Lambda, \zeta_\omega, r] \right\} \\ &\quad - g_\sigma^2 Y[\Lambda, m_\sigma, r], \end{aligned}$$

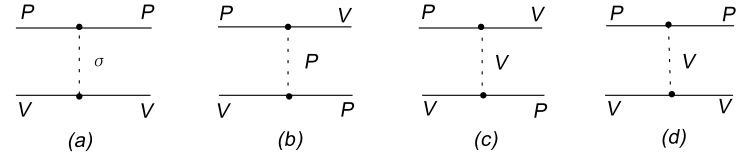
$$\begin{aligned} &- \frac{4}{3} f_{\mathcal{D}^*\mathcal{D}\mathbb{V}}^2 Z[\Lambda, \zeta_\rho, r] + \frac{4}{3} f_{\mathcal{D}^*\mathcal{D}\mathbb{V}}^2 Z[\Lambda, \zeta_\omega, r] \Big\} \\ &- g_\sigma^2 Y[\Lambda, m_\sigma, r]. \end{aligned} \quad (45)$$

For $\Phi^{*0}/\hat{\Phi}^{*0}$, $\Phi_{s1}^{*0}/\hat{\Phi}_{s1}^{*0}$ and $\Phi_8^{*0}/\hat{\Phi}_8^{*0}$, we have

$$\begin{aligned} \mathcal{V}(r)_{\text{Total}}^{\Phi^{*0}/\hat{\Phi}^{*0}} &= \frac{1}{2} g_{\mathcal{D}\mathcal{D}\mathbb{V}} g_{\mathcal{D}^*\mathcal{D}^*\mathbb{V}} \left[\frac{X[\Lambda, m_\rho, r]}{4m_D m_{D^*} m_\rho^2} + Y[\Lambda, m_\rho, r] \right] \\ &\quad - \frac{1}{2} g_{\mathcal{D}\mathcal{D}\mathbb{V}} g_{\mathcal{D}^*\mathcal{D}^*\mathbb{V}} \left[\frac{X[\Lambda, m_\omega, r]}{4m_D m_{D^*} m_\omega^2} + Y[\Lambda, m_\omega, r] \right] \\ &\quad - c \left\{ -\frac{g_{\mathcal{D}^*\mathcal{D}\mathbb{P}}^2}{24m_D m_{D^*}} U(r) - \frac{g_{\mathcal{D}^*\mathcal{D}\mathbb{P}}^2}{72m_D m_{D^*}} Z[\Lambda, \mu', r] \right. \\ &\quad \left. - \frac{4}{3} f_{\mathcal{D}^*\mathcal{D}\mathbb{V}}^2 Z[\Lambda, \zeta_\rho, r] + \frac{4}{3} f_{\mathcal{D}^*\mathcal{D}\mathbb{V}}^2 Z[\Lambda, \zeta_\omega, r] \right\} \\ &\quad - g_\sigma^2 Y[\Lambda, m_\sigma, r], \end{aligned} \quad (46)$$

Table 7 The numerical results for the $\mathcal{D}^* - \bar{\mathcal{D}}^*$ and $\mathcal{B}^* - \bar{\mathcal{B}}^*$ systems after reducing the coupling constants by a factor of two

State	$\mathcal{D}^* - \bar{\mathcal{D}}^*$								
	$J^P = 0^+$			$J^P = 1^+$			$J^P = 2^+$		
	Λ (GeV)	E (MeV)	r_{rms} (fm)	Λ (GeV)	E (MeV)	r_{rms} (fm)	Λ (GeV)	E (MeV)	r_{rms} (fm)
$\Phi_s^{*\pm}(\Phi_s^{*0}, \bar{\Phi}_s^{*0})$	—	—	—	—	—	—	—	—	—
$\Phi^{*\pm}(\Phi^{*0})$	—	—	—	—	—	—	—	—	—
Φ_8^{*0}	0.40 0.41	-18.40 -12.23	1.57 1.81	0.40 0.41	-13.09 -8.43	1.82 2.12	0.39 0.40	-10.14 -6.67	2.10 2.42
Φ_{s1}^{*0}	0.46 0.47	-6.43 -3.70	2.21 2.76	0.40 0.42	-27.87 -16.15	1.37 1.63	0.40 0.41	-12.05 -8.61	1.95 2.18
State	$\mathcal{B}^* - \bar{\mathcal{B}}^*$								
	$J^P = 0^+$			$J^P = 1^+$			$J^P = 2^+$		
	Λ (GeV)	E (MeV)	r_{rms} (fm)	Λ (GeV)	E (MeV)	r_{rms} (fm)	Λ (GeV)	E (MeV)	r_{rms} (fm)
$\mathcal{Q}_s^{*\pm}(\mathcal{Q}_s^{*0}, \bar{\mathcal{Q}}_s^{*0})$	6.80 6.90	-9.33 -23.17	1.43 0.93	—	— —	— —	—	— —	— —
$\mathcal{Q}^{*\pm}(\mathcal{Q}^{*0})$	6.10 6.20	-7.37 -14.64	1.64 1.20	—	— —	— —	—	— —	— —
\mathcal{Q}_8^{*0}	0.48 0.50	-26.88 -8.85	1.31 1.97	0.48 0.50	-19.59 -6.57	1.51 2.25	0.48 0.50	-11.34 -4.18	1.92 2.75
\mathcal{Q}_{s1}^{*0}	0.58 0.60	-11.18 -3.11	1.68 2.85	0.53 0.55	-29.28 -15.49	1.23 1.54	0.50 0.52	-18.73 -9.95	1.60 1.97

Fig. 9 The diagrams in the derivation of the effective potential of the P–V system

$$\begin{aligned} \mathcal{V}(r)_{\text{Total}}^{\Phi_{s1}^{*0}/\hat{\Phi}_{s1}^{*0}} &= -g_{DDV}g_{D^*D^*V} \left[\frac{X[\Lambda, m_\phi, r]}{4m_{D_s}m_{D_s^*}m_\phi^2} + Y[\Lambda, m_\phi, r] \right] \\ &\quad - c \frac{8}{3} f_{D^*D^*V}^2 Z[\Lambda, \zeta_\phi, r] \\ &\quad + c \frac{g_{D^*D^*P}^2}{18m_{D_s}m_{D_s^*}} Z[\Lambda, \mu', r], \end{aligned} \quad (47)$$

$$\begin{aligned} \mathcal{V}(r)_{\text{Total}}^{\Phi_8^{*0}/\hat{\Phi}_8^{*0}} &= -\frac{3}{2} g_{DDV}g_{D^*D^*V} \left[\frac{X[\Lambda, m_\rho, r]}{4m_{Dm_{D^*}}m_\rho^2} + Y[\Lambda, m_\rho, r] \right] \\ &\quad - \frac{1}{2} g_{DDV}g_{D^*D^*V} \left[\frac{X[\Lambda, m_\omega, r]}{4m_{Dm_{D^*}}m_\omega^2} + Y[\Lambda, m_\omega, r] \right] \end{aligned}$$

$$\begin{aligned} &- c \left\{ \frac{g_{D^*D^*P}^2}{8m_D m_{D^*}} U(r) - \frac{g_{D^*D^*P}^2}{72m_D m_{D^*}} Z[\Lambda, \mu', r] \right. \\ &\quad \left. + 4f_{D^*D^*V}^2 Z[\Lambda, \zeta_\rho, r] + \frac{4}{3} f_{D^*D^*V}^2 Z[\Lambda, \zeta_\omega, r] \right\} \\ &\quad - g_\sigma^2 Y[\Lambda, m_\sigma, r]. \end{aligned} \quad (48)$$

The parameter c is ∓ 1 for the P–V systems with the positive and negative charge parity respectively. As expected, the potential of Φ^{*0} and $\hat{\Phi}^{*\pm}$ are the same as that of $\Phi^{*\pm}$ and $\hat{\Phi}^{*0}$ respectively.

6.2 Numerical results for the P–V system

We show the variation of the potential with r in Fig. 10. The total effective potential for $\hat{\Phi}^{*\pm}(\hat{\Phi}^{*0})$ and Φ_8^{*0} is attractive while the potential of $\Phi^{*\pm}(\Phi^{*0})$ and $\hat{\Phi}_8^{*0}$ is repulsive with $\Lambda = 1$ GeV. Especially the neutral states with pos-

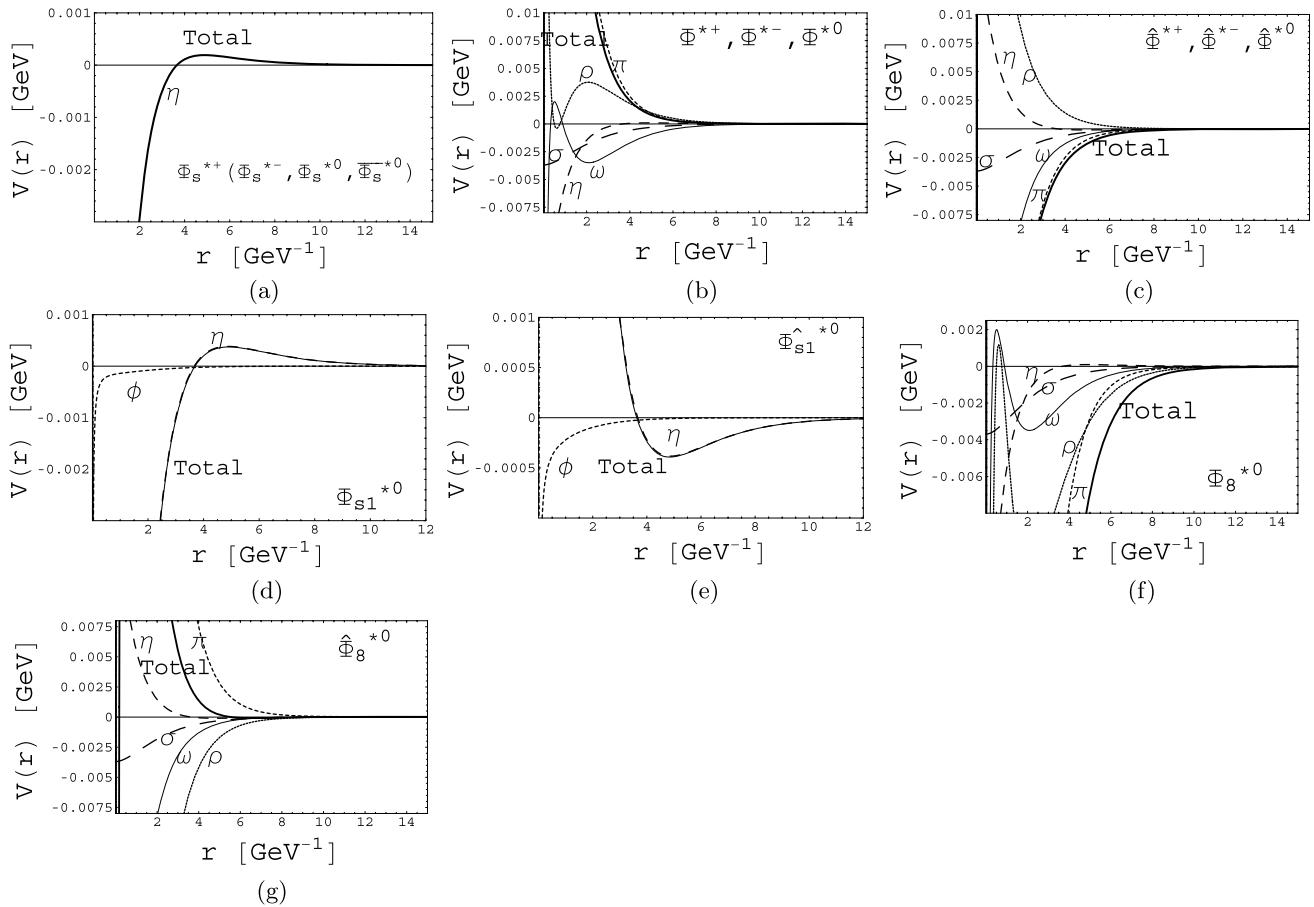


Fig. 10 The exchange potential of the P–V system with the typical value $\Lambda = 1$ GeV. The *thick solid line* is the total effective potential

itive charge parity are very interesting. The only candidate of $X(3872)$ with the attractive potential is Φ_8^{*0} . There do not exist molecular states $\Phi^\pm(\Phi^{*0})$, $\Omega^\pm(\Omega^{*0})$ and $\hat{\Omega}_8^{*0}$ because of the strong repulsive potential. Bound state solutions exist for $\Phi_s^{*\pm}(\Phi_s^{*0}, \bar{\Phi}_s^{*0})$ and $\Omega_s^{*\pm}(\Omega_s^{*0}, \bar{\Omega}_s^{*0})$, $\hat{\Omega}_s^{*\pm}(\hat{\Omega}_s^{*0})$ only with a very large Λ . We show the dependence of the binding energy and r_{rms} of P–V system in Figs. 11–12. Moreover we collect the numerical results in Figs. 11–12 (see the results marked by a yellow shadow band) when all coupling constants are increased by a factor of two. When all the coupling constants are reduced by a factor of two, the results are shown in Table Figs. 11–12 (see the results marked by a blue shadow band).

7 Discussion and conclusion

We have systematically studied the P–P, V–V and P–V systems, which is composed of a pair of heavy meson and anti-meson. We summarize our numerical results from Sects. 4–6 in Tables 8, 9 and 10. We use the symbols ‘✓’ and ‘✗’ to indicate whether a molecular state exists or not with the coupling constants in Sect. 3. In the following two cases,

we tend to label the system with the symbol ‘✗’: (1) there does not exist a bound state at all because of the repulsive potential; (2) a bound state solution exists only with either $\Lambda > 3$ GeV or $\Lambda < 0.5$ GeV. If a bound state exists when $0.5 < \Lambda < 0.9$ GeV or $2.0 < \Lambda < 3.0$ GeV, we mark this state with ‘?’ . In this case the result is so sensitive to the cutoff parameter that we can not draw a definite conclusion. Only when a loosely molecular state exists with $0.9 < \Lambda < 2.0$ GeV, we tend to label the state with the symbol ‘✓’. We want to emphasize that the above criteria may be biased due to the authors’ personal judgement. The readers are encouraged to consult the numerical results in Sects. 4–6 and draw their own conclusions.

It’s interesting to compare our results with those near-threshold structures observed recently.

1. $Z^+(4051)$

The charged broad structure $Z^+(4051)$ was observed by Belle in the $\pi^+\chi_{c1}$. Its central mass value is slightly above the $D^*\bar{D}^*$ threshold. First we want to emphasize that there exists strong attraction in the range $r < 1$ fm for the $D^*\bar{D}^*$ system with $J = 0, 1$ as can be seen

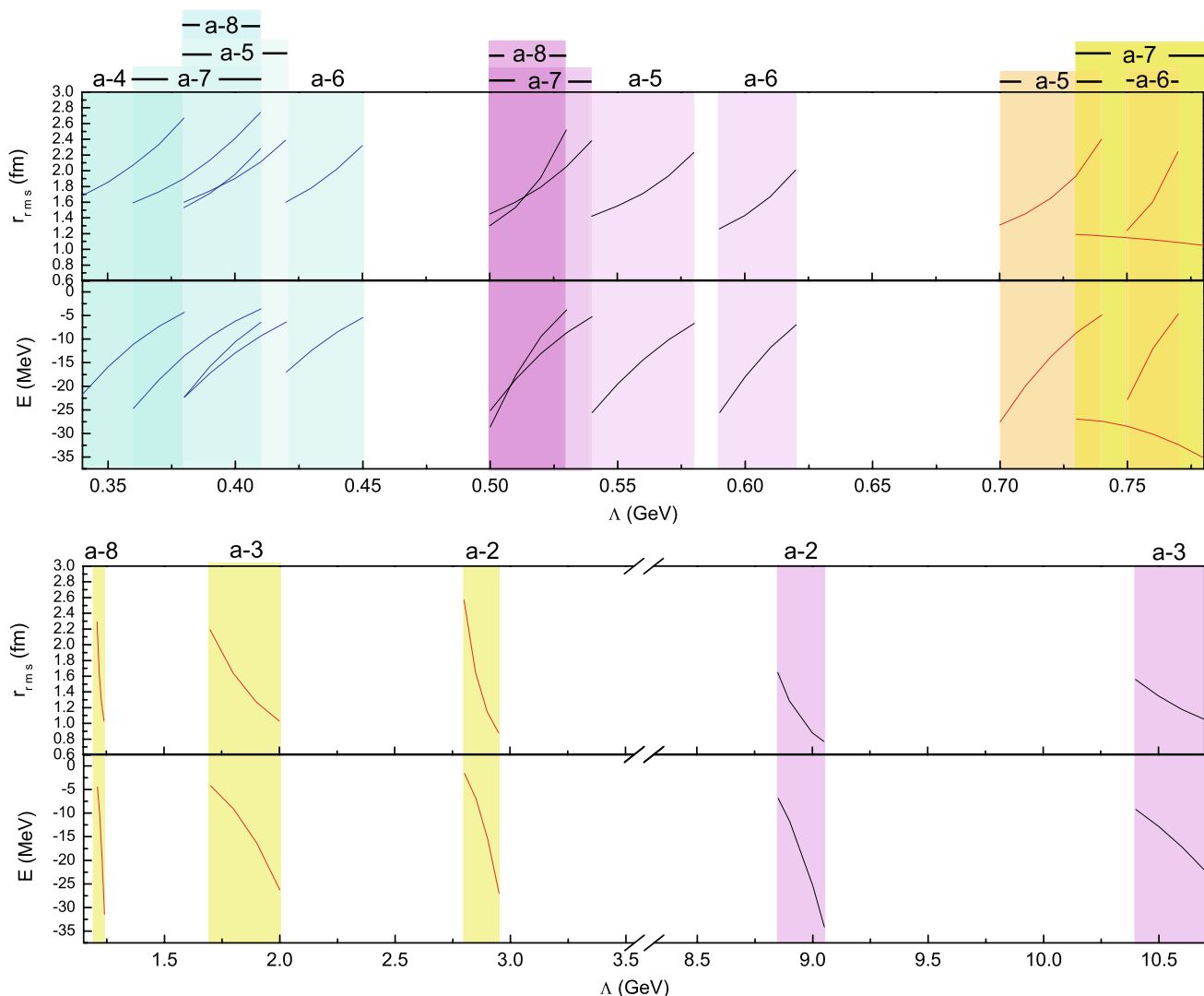


Fig. 11 The dependence of E and r_{rms} on Λ for the case of $D\bar{D}^*$. Here a-2, a-3, a-5, a-6, a-7 and a-8 denote $[\Phi_s^{*\pm}, \Phi_s^{*0}, \bar{\Phi}_s^{*0}]$, $[\hat{\Phi}^{*\pm}, \hat{\Phi}^{*0}]$, $[\Phi_{s1}^{*0}]$, $[\hat{\Phi}_{s1}^{*0}]$, $[\Phi_8^{*0}]$ and $[\hat{\Phi}_8^{*0}]$ respectively. The other conventions are the same as in Fig. 3

clearly from the shape of the total effective potential in Fig. 5(a)–(b).

If this enhancement is a molecular state, the potential candidate of $Z^+(4051)$ is the Φ^{***+} state with isospin $I = 1$. Our numerical results indicate that there exists a bound state solution (1) for Φ^{***+} with $J^P = 0^+$ and $\Lambda \sim 4$ GeV; (2) for Φ^{***+} with $J^P = 1^+$ and $\Lambda \sim 10$ GeV. Unfortunately such a cutoff seems too large according to our criteria.

If future experiments confirm $Z^+(4051)$ as a loosely bound molecular state, its quantum number is very probably $J^P = 0^+$, which can be measured experimentally through the angular momentum distribution of $\pi^+\chi_{c1}$. Since Φ^{***+} belongs to an isospin triplet, its neutral partner state Φ^{**0} may be searched in the $\pi^0\chi_{c1}$ channel.

2. $X(3872)$

In our previous work [17, 18], we explored the $D^0\bar{D}^{*0}$ molecular state by considering the π and σ meson exchange potentials only. Our numerical results showed that it is impossible to form a $D^0\bar{D}^{*0}$ molecular state with the coupling constants determined by experiment and a reasonable cutoff around 1 GeV [17, 18]. Unfortunately we missed a minus sign in the sigma meson exchange potential, although its contribution is not large. Moreover we didn't take into account the charged modes.

In this work, we consider both the neutral and charged modes and include the exchange force from the π , η , σ , ρ and ω mesons. The resulting total effective potential is attractive as shown in Fig. 10(f). Vector meson exchange, especially rho meson exchange, provides the

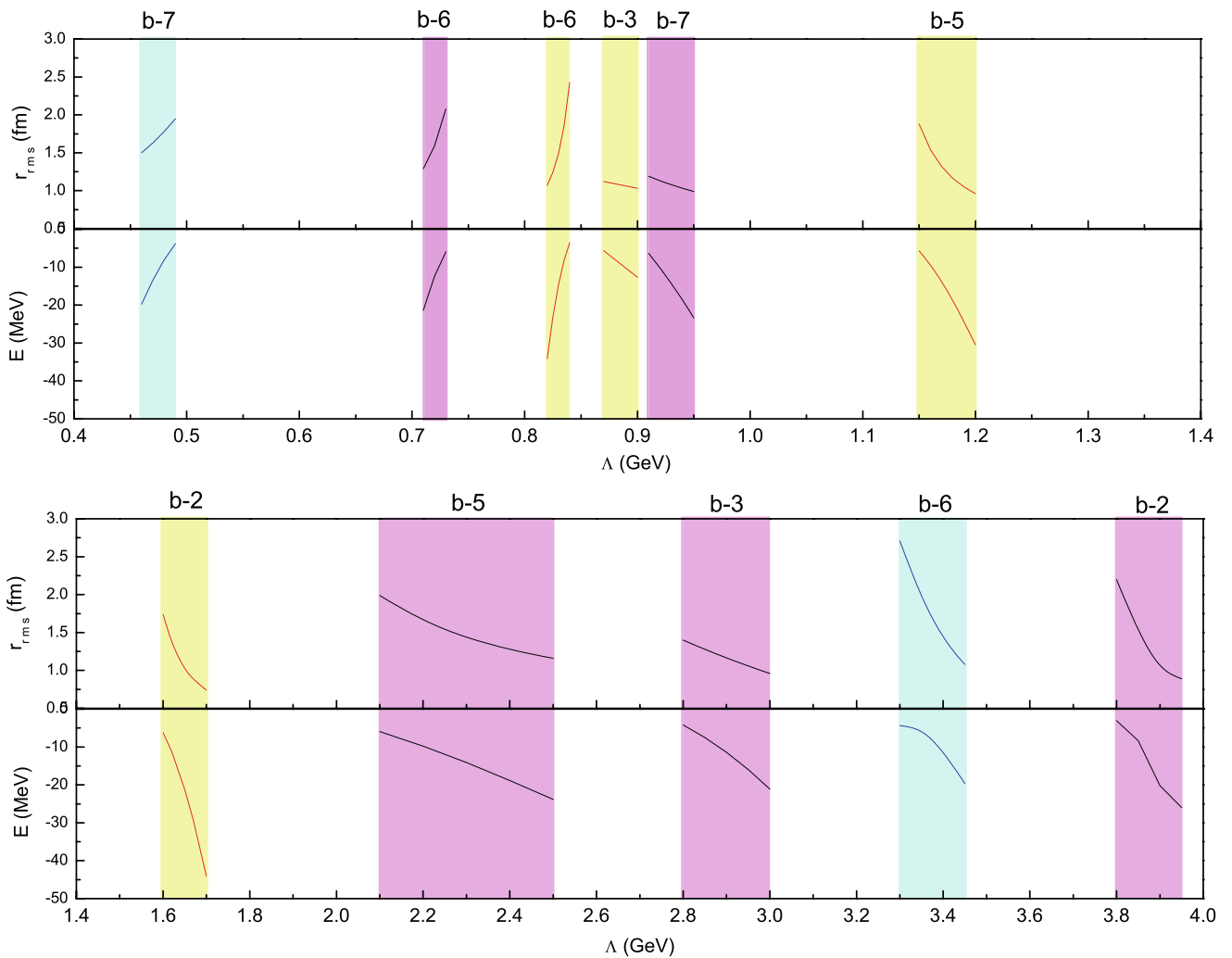


Fig. 12 The dependence of E and r_{rms} on Λ for the case of $B\bar{B}^*$. Here b-2, b-3, b-5, b-6 and b-7 denote $[\Omega_s^{*\pm}, \Omega_s^{*0}, \bar{\Omega}_s^{*0}]$, $[\hat{\Omega}^{*\pm}, \hat{\Omega}^{*0}]$, $[\Omega_{s1}^{*0}]$, $[\hat{\Omega}_{s1}^{*0}]$ and $[\mathcal{Q}_8^{*0}]$ respectively. The other conventions are the same as that in Fig. 3

additional strong attraction. The Φ_8^{*0} state corresponds the $X(3872)$.

Recall that the sigma meson exchange force is weak and pion meson exchange alone does not bind the $D^*\bar{D}$ into a molecular state with a physical pionic coupling constant and a reasonable cutoff [17, 18]. In fact, a bound state appears only with $\Lambda \sim 6$ GeV there. With the additional strong attraction from vector meson exchange, our present numerical analysis shows that a molecular state exists with $\Lambda \sim 0.55$ GeV. If we arbitrarily increase all the coupling constants by a factor of two, there exists a molecular state with a slightly more reasonable $\Lambda \sim 0.75$ GeV. If we reduce all the coupling constants by a factor two, there appears a bound state with $\Lambda \sim 0.45$ GeV. Such a cutoff value is below 1 GeV and smaller than the exchanged vector meson mass.

The pionic coupling constant of the $D^*\bar{D}$ system was extracted from the decay width of the D^* meson experi-

Table 8 Summary of the $D - \bar{D}$ and $B - \bar{B}$ systems. The symbols \otimes and \checkmark denote “forbidden” and “allowed” respectively

$D - \bar{D}$		$B - \bar{B}$	
State	Remark	State	Remark
$\Phi_s^{\pm}, \Phi_s^0, \bar{\Phi}_s^0$	\otimes	$\Omega_s^{\pm}, \Omega_s^0, \bar{\Omega}_s^0$	\otimes
Φ^{\pm}, Φ^0	\otimes	Ω^{\pm}, Ω^0	\otimes
Φ_8^0	?	Ω_8^0	\checkmark
Φ_{s1}^0	?	Ω_{s1}^0	?

mentally. Its value is known quite reliably. In contrast, the vector coupling constant was estimated using the vector dominance model in [41], which may be overestimated according to a recent light cone QCD sum rule analysis [45]. If we fix the pionic and scalar coupling constants but reduce the vector coupling by a factor of two only, there exists a very reasonable bound state solution

Table 9 Summary of the $\mathcal{D}^* - \bar{\mathcal{D}}^*$ and $\mathcal{B}^* - \bar{\mathcal{B}}^*$ systems

$\mathcal{D}^* - \bar{\mathcal{D}}^*$					$\mathcal{B}^* - \bar{\mathcal{B}}^*$	
State	Remark	$J^P = 0^+$ $J^P = 1^+$ $J^P = 2^+$			State	Remark
		$J^P = 0^+$	$J^P = 1^+$	$J^P = 2^+$		
$\Phi_s^{*\pm}, \Phi_s^{*0}, \bar{\Phi}_s^{*0}$	\otimes	\otimes	\otimes	\otimes	$\Omega_s^{*\pm}, \Omega_s^{*0}, \bar{\Omega}_s^{*0}$?
$\Phi^{*\pm}, \Phi^{*0}$	\otimes	\otimes	\otimes	\otimes	$\Omega^{*\pm}, \Omega^{*0}$	✓
Φ_8^{*0}	?	?	?	?	Ω_8^{*0}	?
Φ_{s1}^{*0}	?	?	?	?	Ω_{s1}^{*0}	?

Table 10 Summary of the $\mathcal{D} - \bar{\mathcal{D}}^*$ and $\mathcal{B} - \bar{\mathcal{B}}^*$ systems

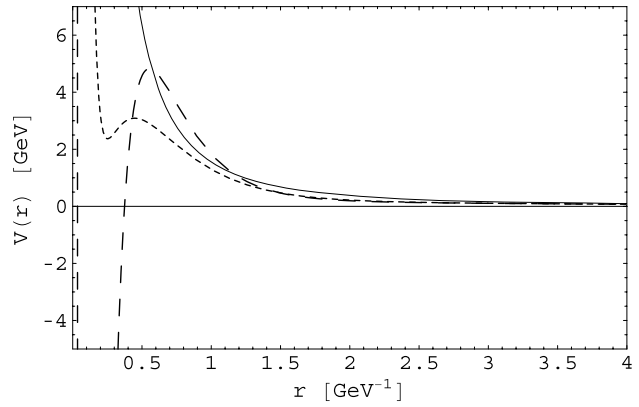
$\mathcal{D} - \bar{\mathcal{D}}^*$		$\mathcal{B} - \bar{\mathcal{B}}^*$	
State	Remark	State	Remark
$\Phi_s^{*\pm}, \Phi_s^{*0}, \bar{\Phi}_s^{*0}$	\otimes	$\Omega_s^{*\pm}, \Omega_s^{*0}, \bar{\Omega}_s^{*0}$	\otimes
$\hat{\Phi}_s^{*\pm}, \hat{\Phi}_s^{*0}, \hat{\bar{\Phi}}_s^{*0}$	\otimes	$\hat{\Omega}_s^{*\pm}, \hat{\Omega}_s^{*0}, \hat{\bar{\Omega}}_s^{*0}$	\otimes
$\Phi^{*\pm}, \Phi^{*0}$	\otimes	$\Omega^{*\pm}, \Omega^{*0}$	\otimes
$\hat{\Phi}^{*\pm}, \hat{\Phi}^{*0}$	\otimes	$\hat{\Omega}^{*\pm}, \hat{\Omega}^{*0}$	\otimes
Φ_{s1}^{*0}	?	Ω_{s1}^{*0}	?
$\hat{\Phi}_{s1}^{*0}$?	$\hat{\Omega}_{s1}^{*0}$?
Φ_8^{*0}	?	Ω_8^{*0}	✓
$\hat{\Phi}_8^{*0}$?	$\hat{\Omega}_8^{*0}$	\otimes

Table 11 The bound state solutions for the $D^* - \bar{D}$ system if we fix the pionic and scalar coupling constants and reduce only the vector coupling constant in Sect. 3 by a factor of two

Λ	E (MeV)	r_{rms} (fm)
1.6	-12.86	1.47
1.5	-6.07	1.98
1.42	-2.41	3.09
1.41	-2.07	3.30
1.40	-1.75	3.53

with $E = -1.75$ GeV and $\Lambda = 1.4$ GeV as shown in Table 11. Now the value of its root-mean-square radius reaches 3.53 fm! In other words, such a molecular state is bound very loosely.

In short summary, $X(3764)$ may be accommodated as a molecular state dynamically, although drawing a very definite conclusion is very difficult especially when other available experimental information is taken into account. In our calculation, we assumed the SU(2) symmetry and ignored the mass difference between the charged and neutral mesons. Moreover we ignored the possible S–D mixing effect completely since we impose the S-wave condition in the derivation of the potential. These approximations together with the sensitivity of the numerical re-

**Fig. 13** The dependence of the potential $V(r)^{\phi_8^0}_{\text{Total}} + 3/(2\mu r^2)$ on Λ . The solid, dotted and dashed lines correspond to $\Lambda = 1, 3, 4$ GeV respectively

sults to the cutoff parameter should be considered in the future investigation.

3. $X(3764)$

The broad structure $X(3764)$ is close to the $D\bar{D}$ threshold and was observed in $e^+e^- \rightarrow \text{hadrons}$ process. Its quantum number is $J^P = 1^{--}$. In the present case, we need consider the P-wave Φ_8^0 by adding the centrifugal potential $\ell(1+\ell)/(2\mu r^2)$ with $\ell = 1$ into the potential in (19). Here μ is the reduced mass of the system. In Fig. 13, we show the variation of $V(r)^{\phi_8^0}_{\text{Total}} + 3/(2\mu r^2)$ with several typical values of Λ . Our numerical analysis indicates that there does not exist a P-wave Φ_8^0 from such a potential. In other words, the structure $X(3764)$ is not a $D\bar{D}$ molecular state.

Acknowledgements The authors thank Professors K.T. Chao and Z.Y. Zhang for helpful discussions. This project was supported by National Natural Science Foundation of China under Grants 10625521, 10675008, 10705001, 10775146, 10721063 and China Postdoctoral Science foundation (20070420526). One of authors (X.L.) thanks the support by the Fundação para a Ciência e a Tecnologia of the Ministério da Ciência, Tecnologia e Ensino Superior of Portugal (SFRH/BPD/34819/2007).

References

1. K. Abe et al. (Belle Collaboration), Phys. Rev. Lett. **100**, 142001 (2008)
2. R. Mizuk et al. (Belle Collaboration), arXiv:0806.4098 [hep-ex]
3. M. Ablikim et al. (BES Collaboration), arXiv:0807.0494 [hep-ex]
4. M.B. Voloshin, L.B. Okun, JETP Lett. **23**, 333 (1976)
5. A.D. Rujula, H. Georgi, S.L. Glashow, Phys. Rev. Lett. **38**, 317 (1977)
6. N.A. Törnqvist, Nuovo Cim. A **107**, 2471–2476 (1994)
7. N.A. Törnqvist, Z. Phys. C **61**, 525–537 (1994)
8. M.B. Voloshin, arXiv:hep-ph/0602233
9. S. Dubynskiy, M.B. Voloshin, Mod. Phys. Lett. A **21**, 2779 (2006)
10. Y.J. Zhang, H.C. Chiang, P.N. Shen, B.S. Zou, Phys. Rev. D **74**, 014013 (2006)
11. F.E. Close, P.R. Page, Phys. Lett. B **578**, 119 (2004)
12. M.B. Voloshin, Phys. Lett. B **579**, 316 (2004)
13. C.Y. Wong, Phys. Rev. C **69**, 055202 (2004)
14. E.S. Swanson, Phys. Lett. B **588**, 189 (2004)
15. E.S. Swanson, Phys. Lett. B **598**, 197 (2004)
16. N.A. Törnqvist, Phys. Lett. B **590**, 209 (2004)
17. Y.R. Liu, X. Liu, W.Z. Deng, S.L. Zhu, arXiv:0801.3540 [hep-ph]
18. Y.R. Liu, X. Liu, W.Z. Deng, S.L. Zhu, Eur. Phys. J. C **56**, 63 (2008)
19. X. Liu, Y.R. Liu, W.Z. Deng, arXiv:0802.3157
20. Y.R. Liu, Z.Y. Zhang, arXiv:0805.1616 [hep-ph]
21. C.E. Thomas, F.E. Close, arXiv:0805.3653 [hep-ph]
22. J.L. Rosner, Phys. Rev. D **76**, 114002 (2007)
23. C. Meng, K.T. Chao, arXiv:0708.4222 [hep-ph]
24. X. Liu, Y.R. Liu, W.Z. Deng, S.L. Zhu, Phys. Rev. D **77**, 034003 (2008)
25. X. Liu, Y.R. Liu, W.Z. Deng, S.L. Zhu, arXiv:0711.0494 [hep-ph]
26. X. Liu, Y.R. Liu, W.Z. Deng, S.L. Zhu, Phys. Rev. D **77**, 094015 (2008)
27. X. Liu, Y.R. Liu, W.Z. Deng, S.L. Zhu, arXiv:0803.1295 [hep-ph]
28. W.M. Yao et al. (Particle Data Group), J. Phys. G **33**, 1 (2006)
29. M.P. Locher, Y. Lu, B.S. Zou, Z. Phys. A **347**, 281 (1994)
30. X.Q. Li, D.V. Bugg, B.S. Zou, Phys. Rev. D **55**, 1421 (1997)
31. X.G. He, X.Q. Li, X. Liu, X.Q. Zeng, Eur. Phys. J. C **51**, 883–889 (2007)
32. X.G. He, X.Q. Li, X. Liu, X.Q. Zeng, arXiv:hep-ph/0606015
33. X. Liu, X.Q. Zeng, X.Q. Li, Phys. Rev. D **74**, 074003 (2006)
34. X. Liu, X.Q. Zeng, X.Q. Li, arXiv:hep-ph/0606191
35. H.Y. Cheng, C.Y. Cheung, G.L. Lin, Y.C. Lin, T.M. Yan, H.L. Yu, Phys. Rev. D **47**, 1030 (1993)
36. T.M. Yan, H.Y. Cheng, C.Y. Cheung, G.L. Lin, Y.C. Lin, H.L. Yu, Phys. Rev. D **46**, 1148 (1992)
37. M.B. Wise, Phys. Rev. D **45**, R2188 (1992)
38. G. Burdman, J. Donoghue, Phys. Lett. B **280**, 287 (1992)
39. R. Casalbuoni, A. Deandrea, N. Di Bartolomeo, R. Gatto, F. Feruglio, G. Nardulli, Phys. Rep. **281**, 145 (1997)
40. A.F. Falk, M. Luke, Phys. Lett. B **292**, 119 (1992)
41. C. Isola, M. Ladisa, G. Nardulli, P. Santorelli, Phys. Rev. D **68**, 114001 (2003)
42. V. Ledoux, M.V. Daele, G.V. Berghe, Comput. Phys. Commun. **162**, 151 (2004)
43. V. Ledoux, M.V. Daele, G.V. Berghe, ACM Trans. Math. Softw. **31**, 532–554 (2005)
44. V. Ledoux, M.V. Daele, G.V. Berghe, <http://users.ugent.be/~vledoux/MATSLISE/>
45. Z.H. Li, W. Liu, H.Y. Liu, Phys. Lett. B **659**, 598 (2008)